Regional mid-Pleistocene glaciation in central Patagonia

DOI:
10.1016/j.quascirev.2017.03.023

Document Version
Accepted author manuscript

Regional mid-Pleistocene glaciation in central Patagonia

Andrew S. Hein[1*], Antoine Cogez[2], Christopher M. Darvill[3], Monika Mendelova[1], Michael R. Kaplan[4], Frédéric Herman[2], Tibor J. Dunai[5], Kevin Norton[6], Sheng Xu[7], Marcus Christl[8], Angel Rodés[7]

[1]*School of GeoSciences, University of Edinburgh, Drummond Street, Edinburgh, EH8 9XP, UK*
[2]*Institute of Earth Surface Dynamics, University of Lausanne, Geopolis, CH-1015 Lausanne, Switzerland*
[3]*Geography Program and Natural Resources and Environmental Studies Institute, University of Northern British Columbia, Prince George, Canada*
[4]*Geochemistry, Lamont-Doherty Earth Observatory, Geochemistry, Palisades, New York 10964, USA*
[5]*Institute for Geology and Mineralogy, University of Cologne, Cologne, Germany*
[6]*School of Geography, Environment, and Earth Sciences, Victoria University of Wellington, Wellington, New Zealand*
[7]*Scottish Universities Environmental Research Centre, Rankine Avenue, East Kilbride, G75 0QF, UK*
[8]*Ion Beam Physics Laboratory, Swiss Federal Institute of Zürich, Zürich, Switzerland*

** Corresponding author: Andy.Hein@ed.ac.uk*

Abstract

Southern South America contains a glacial geomorphological record that spans the past million years and has the potential to provide palaeoclimate information for several glacial periods in Earth's history. In central Patagonia, two major outlet glaciers of the former Patagonian Ice Sheet carved deep basins ~50 km wide and extending over 100 km into the Andean plain east of the mountain front. A succession of nested glacial moraines offers the possibility of determining when the ice lobes advanced and whether such advances occurred synchronously. The existing chronology, which was obtained using different methods in each valley, indicates the penultimate moraines differ in age by a full glacial cycle. Here, we test this hypothesis further using a uniform methodology that combines cosmogenic nuclide ages from moraine boulders, moraine cobbles and outwash cobbles. ^{10}Be concentrations in eighteen outwash cobbles from the Moreno outwash terrace in the Lago Buenos Aires valley yield surface exposure ages of 169-269 ka. We find ^{10}Be inheritance is low and therefore use the oldest surface cobbles to date the deposit at 260-270 ka, which is indistinguishable

from the age obtained in the neighbouring Lago Pueyrredón valley. This suggests a regionally significant glaciation during Marine Isotope Stage 8, and broad interhemispheric synchrony of glacial maxima during the mid to late Pleistocene. Finally, we find the dated outwash terrace is 70-100 ka older than the associated moraines. On the basis of geomorphological observations, we suggest this difference can be explained by exhumation of moraine boulders.

Keywords: Cosmogenic nuclide surface exposure dating; Marine Isotope Stage 8; Glacial chronology; moraine degradation; Beryllium-10; Last Glacial Maximum; moraine boulders.

1. Introduction

The glacial geomorphological record in southernmost South America is well preserved and reflects advances of the former Patagonian Ice Sheet over at least the past million years. The location of Patagonia in the mid-latitudes of the southern hemisphere makes it ideal for investigating interhemispheric leads and lags in the timing of glacial advances (Denton et al., 1999a; Kaplan et al., 2004), with implications for the mechanisms that drive global climate changes (Blunier and Brook, 2001; Blunier et al., 1997; Darvill et al., 2016; Moreno et al., 2009; Pedro et al., 2016). Efforts to exploit the palaeoclimatic significance of this record have largely focused on the last glacial cycle (e.g., Denton et al., 1999b; Douglass et al., 2005; Garcia et al., 2012; Glasser et al., 2008; Hein et al., 2010; Kaplan et al., 2004; McCulloch et al., 2005), since the landforms are better preserved and within the age-range of common geochronometers. While knowledge of the most recent glaciation and deglaciation in Patagonia is improving, comparatively little is known about earlier glaciations in the region; this despite the preservation of pre-Last Glacial Maximum (LGM) moraine systems and their value in providing insight into southern mid-latitude palaeoclimate throughout the Quaternary period.

In Argentine Patagonia, valleys that were formerly occupied by glaciers draining the Patagonian Ice Sheet often contain several Quaternary moraine and outwash terrace assemblages (Caldenius, 1932; Clapperton, 1993; Coronato et al., 2004; Glasser et al., 2008; Kaplan et al., 2009). Constraints on the ages of older deposits are, in general, restricted to a few locations where lava flows bracket glacial till sediments. Here, K-Ar or $^{40}Ar/^{39}Ar$ dating of the lava flows can yield limiting ages and morphostratigraphy, which links the relative order of neighbouring landforms, has been used to correlate different moraine systems over hundreds of kilometres (Coronato et al., 2004; Rabassa and Clapperton, 1990; Singer et al., 2004). The technique has been instrumental in establishing the early onset of glaciation in Patagonia at least by 7-5 Ma, and in determining the age of the most extensive Quaternary deposits of the 'Greatest Patagonian Glaciation', dated at ~1.1 Ma (Meglioli, 1992; Mercer, 1976; Rabassa and

Clapperton, 1990; Rabassa et al., 2000; Singer et al., 2004; Ton-That et al., 1999). However, age correlations based on morphostratigraphy alone are open to conjecture given that preservation of different-aged glacial sediments in neighbouring valleys is not uncommon (e.g., Putnam et al., 2013; Schaefer et al., 2015). Consequently, direct dating of individual moraine limits is required to make correlations between areas and to exploit fully the geomorphological record and enable palaeoclimate inferences to be drawn.

Efforts to date pre-LGM glacial sediments in the region have involved a range of techniques including soil formation rates (Douglass and Bockheim, 2006), ^{230}Th/U disequilibria dating of soil carbonate (Phillips et al., 2006), optically stimulated luminescence (Smedley et al., 2016), and cosmogenic nuclide surface exposure dating (Darvill et al., 2015b; Hein et al., 2011; Hein et al., 2009; Kaplan et al., 2005). Unlike the other techniques, cosmogenic nuclide surface exposure dating has the potential to directly-date moraine surfaces that are millions of years old. However, pre-LGM landforms can degrade through time, meaning surface exposure ages can underestimate the moraine age (Hallet and Putkonen, 1994; Heyman et al., 2011; Putkonen and O'Neal, 2006; Putkonen and Swanson, 2003). In addition, boulder surface erosion is difficult to quantify, especially if exhumed at an unknown time, and becomes an increasing source of uncertainty with age. Consequently, the combination of boulder exhumation and variable rock (i.e., boulder/cobble) surface erosion can cause wide scatter in exposure ages from old moraines (Balco, 2011; Kaplan et al., 2007; Phillips et al., 1990).

Hein et al. (2009; 2011) demonstrated that surface exposure dating of outwash gravels rather than moraine boulders could provide robust age constraints for pre-LGM moraine systems in central Patagonia. Exhumation and rock surface erosion are limited by sampling fluvial cobbles from outwash plains linked to moraine limits; the rounded fluvial shape indicates negligible rock surface erosion and exhumation is minimised by sampling from flat surfaces as opposed unconsolidated moraines with steeper slope morphology. In the Lago Pueyrredón (LP) valley (Fig. 1), Hein et al. (2009) demonstrated that ^{10}Be concentrations in outwash sediments from the penultimate moraine sequence

(Hatcher moraines) were deposited at *ca.* 260 ka. This was more than 100 ka earlier than the age implied by the corresponding moraine boulders. Darvill et al. (2015b) used the same approach to date the Río Cullen and San Sebastián glacial limits of the former Bahía Inútil-San Sebastián ice lobe on Tierra del Fuego at *ca.* 45 ka and 30 ka, indicating a significant advance during Marine Isotope Stage (MIS) 3. These studies have demonstrated that surface exposure dating of outwash sediments to gauge the timing of glacial activity is effective over a range of timescales pertinent to glacial geochronology in southern South America.

This study uses the outwash cobble approach to date the penultimate moraine sequence in the Lago Buenos Aires (LBA) valley (Fig. 1). Like the neighbouring LP valley, a major outlet glacier of the former Patagonian Ice Sheet carved this valley and left behind a sequence of nested glacial moraines. Given the broad similarity between these two valleys, and that they both share a common accumulation drainage area of the former ice sheet, the morphostratigraphy would suggest the penultimate moraines ('Moreno' and 'Hatcher', respectively) are age-equivalent, but existing geochronological data conflict. We aim to determine whether these moraines represent a correlated regional advance of the Patagonian Ice Sheet or asynchronous behaviour between two large adjacent outlet lobes.

2. Regional Setting

The LBA valley, 46.5° S, Argentina, is located in central Patagonia just north of the LP valley. The valley trends west-east, with a glacial over-deepening that separates the Miocene to Pliocene-aged volcanic plateau of the Meseta del Lago Buenos Aires to the south from the sedimentary deposits of the Meseta del Guenguel to the north (Fig. 1). The valley aligns in part with known faults in the region (Lagabrielle et al., 2007; Lagabrielle et al., 2004; Scalabrino et al., 2010). Quaternary glacial and glaciofluvial sediments dominate the geology east of LBA lake (Caldenius, 1932). To the west, Jurassic volcaniclastic rocks overly Palaeozoic basement rocks, which in turn have been intruded by the late

Jurassic-Miocene Patagonian Batholith (Scalabrino et al., 2010; Suárez and De La Cruz, 2001). This zone, more than 100 km west of the moraines, is thought to be the primary source of quartz cobbles found in the Quaternary sediments.

The climate is dominated by the influence of the southern hemisphere westerly winds, which bring significant precipitation that can exceed 8,000 mm a^{-1} on the western side of the Andes (Carrasco et al., 2002; Garreaud et al., 2013). In contrast, the eastern side of the Andes is semi-arid with precipitation as low as 200 mm a^{-1} east of LBA, some 80 km from the mountain front (Prohaska, 1976). This precipitation gradient, amplified during glacial periods by the presence of the Patagonian Ice Sheet (Hulton et al., 1994; Hulton et al., 2002), is partly responsible for the exceptional preservation of the moraine record. Annual snow cover is thin and intermittent, and would likely not have increased significantly during glacial periods due to the development of the ice sheet. Winds are strong and persistent and play a demonstrable but relatively slow role in rock surface erosion (Ackert and Mukhopadhyay, 2005; Douglass et al., 2007; Hein et al., 2011; Hein et al., 2009; Kaplan et al., 2007; Kaplan et al., 2005). Moraine boulders commonly exhibit ventifacts and flutings while cobbles on outwash terraces often possess rock varnish on ventifacts; the latter suggests aeolian erosion was not recent, or pervasive enough to remove the varnish. Field observations indicate a lack of debris in winds of at least 10 m s^{-1}, thus confirming that such erosion is not occurring today in a widespread manner.

The moraine sequences east of LBA have been extensively mapped (Caldenius, 1932; Kaplan et al., 2005; Mörner and Sylwan, 1989; Singer et al., 2004; Smedley et al., 2016). Based on the pioneering work of Caldenius (1932), four broadly defined glacial moraine systems are distinguished over a distance of 50 km, with the innermost deposits situated ~200 m lower in elevation than the outermost (Figs. 1-3). These systems were informally named (Singer et al., 2004) Fenix, Moreno, Deseado and Telken, from youngest to oldest, respectively, and a prominent escarpment of 30-80 m separates each system. During glacial maxima, meltwater discharged directly onto broad outwash plains until the ice retreated and pro-glacial lakes formed, dammed by terminal moraines. River

185 incision in response to decreased sediment load (cf. Chorley et al., 1984) led to
186 the abandoning of outwash plains and the formation of stable outwash terraces.
187 We infer the outwash terraces stabilized shortly after glacial maximum
188 conditions.
189
190 **2.1 Existing glacial chronology**
191
192 Cosmogenic ^{10}Be, ^{26}Al, and ^{3}He exposure age dating of the Fenix moraine system
193 indicate deposition during the local LGM at *ca.* 26–18 ka (Ackert et al., 2003;
194 Douglass et al., 2006; Kaplan et al., 2004; Kaplan et al., 2011). The chronology for
195 the older moraine systems in the LBA valley spans the past million years as
196 indicated by K-Ar and ^{40}Ar/^{39}Ar ages from three lava flows that over- or underlie
197 glacial till (Mercer, 1976; Singer et al., 2004; Ton-That et al., 1999),
198 magnetostratigraphy (Mörner and Sylwan, 1989), and cosmogenic nuclide data
199 (Kaplan et al., 2005)(Fig. 1).
200
201 **2.1.1 Existing age constraints for the Moreno moraines (LBA valley)**
202
203 Kaplan et al. (2005) measured cosmogenic ^{10}Be and ^{26}Al in moraine boulders to
204 determine the age of the Moreno I-III and Deseado I moraines (Figs. 2-3). The
205 exposure ages are scattered, but there is some consistency in the age ranges and
206 the oldest ages obtained for the Moreno I and II moraines. Twelve boulders from
207 these two moraines revealed similar age ranges that together spanned 153-74 ka
208 assuming no rock surface erosion (i.e., minimum ages). One younger sample
209 returned an age of *ca.* 40 ka (LBA-02-25; 25 cm boulder height). In this valley,
210 Kaplan et al. (2005) estimated a *maximum* erosion rate of 1.4 m Ma^{-1} for
211 boulders, which increased the age range to 190-92 ka. This was considered a
212 maximum erosion rate because it was derived from old (>760 ka) moraine
213 boulders and thus makes assumptions about their exposure and fracture history;
214 it was also not clear whether spatially constant erosion was reasonable in the
215 valley. Indeed, Douglass et al. (2007) further constrained the boulder erosion
216 rate to about 0.2 m Ma^{-1} (range 0.0-4.6 m Ma^{-1}) based on paired ^{36}Cl/^{10}Be
217 concentrations. Kaplan et al. (2005) used two interpretive approaches to

estimate the age of the Moreno I and II moraines, the oldest boulder age assuming no rock surface erosion (cf. Zreda and Phillips, 1995) and the average of all boulder ages with an erosion rate applied. These two approaches yielded consistent results, leading Kaplan et al. (2005) to suggest an age for Moreno I and II of *ca.* 150-140 ka, or MIS 6. This conclusion of an MIS 6 advance does not change with the more recently derived, lower production rates (Kaplan et al., 2011). The interpreted age is consistent with the minimum bracketing age of 109±3 ka for the Cerro Volcán flow. The age of the Moreno III and Deseado I moraines is comparatively uncertain, but is younger than the 760 ka Arroyo Page Flow (Fig. 1). Exposure dates from these moraines are more scattered, with three of seven boulders giving significantly older ages > 270 ka, leading Kaplan et al. (2005) to suggest an MIS 8 or older age for the Moreno III and Deseado I moraines.

There are other lines of evidence that have supported a MIS 6 age for the Moreno moraines. ^{230}Th/U disequilibria dating of soil carbonate formed in outwash gravels associated with the Moreno II moraine suggest onset of calcic pedogenesis at 170±8.3 ka (Phillips et al., 2006). Assuming no carbonate dissolution had occurred subsequently, and the carbonate formation has been continuous without interruption, then these data support the ages from the moraine boulders. Finally, a recent study applied optically stimulated luminescence (OSL) ages determined using single grains of K-feldspar from proglacial outwash sediments (Smedley et al., 2016). These data suggest major glaciolacustrine and glaciofluvial accumulations incorporated within the Moreno I, III and Deseado II moraine limits occurred at around 140±20 ka to 110±20 ka, implying a MIS 6 age for both the Moreno and Deseado moraine systems (Fig. 3).

2.1.2 Existing age constraints for the Hatcher moraines (LP Valley)

Hein et al. (2009) obtained scattered ^{10}Be exposure ages of 153-95 ka from four moraine boulders on the Hatcher moraines, a result that mirrors the boulder ages from the Moreno moraines. On their own, these data suggest a deposition age of *ca.* 150 ka. However, subsequent dating of seven outwash cobbles on the

Hatcher outwash terrace yielded much older exposure ages ranging from 265-194 ka (Hein et al., 2009). An accompanying depth-profile through the outwash terrace confirmed this old age and indicated a low terrace erosion rate of *ca.* 0.53 m Ma^{-1}, equivalent to about 14 cm of surface lowering. The scatter in the surface cobble ages was interpreted to reflect continuous exposure of the oldest clasts, and recent bio- or cryo-turbation of the youngest clasts from the upper 10 cm of the deposit. With inheritance demonstrably negligible, the oldest surface cobbles were used to date the deposit at 260.6±6.5 ka (1σ external ±34 ka).

The cause of the erroneously young moraine boulders was attributed to exhumation as a consequence of moraine degradation. Five moraine cobbles with rounded to subrounded shapes (i.e., negligible rock surface erosion) were sampled from the same moraines as the boulders. These yielded much younger exposure ages of 58-42 ka, a likely consequence of greater exhumation of the smaller cobbles. As such, the concentrations may better reflect moraine degradation rates. The low ^{10}Be concentrations could be achieved with a continuous moraine degradation rate of 12 m Ma^{-1}, equating to ~3 m of surface lowering over the 260 ka exposure time.

3. Approach and Methodology

To determine the age of the Moreno moraine system we mapped and dated outwash sediment associated with the moraine limits and compared our results to existing data. Fieldwork was conducted in 2009, 2012 and 2015 by two separate sub-groups, and the cosmogenic nuclide samples were prepared and measured at three different wet-chemical preparation and AMS laboratories.

3.1 Sampling approach

Where possible, samples were collected from outwash terraces that could be traced and thus corresponded to dated moraines (Figs. 2, 4-5). We avoided locations where older moraine or outwash material could have been incorporated into younger outwash. Outwash cobbles of quartz or quartz-rich

lithologies (5-20 cm long axis) were sampled because such clasts are resistant to weathering. We preferentially targeted cobbles that contained ventifacts and/or rock varnish as evidence for long surface exposure (Fig. 5). The clasts were collected from flat terrace surfaces that were far away from moraines and scarps. We collected one sample from the Fenix V outwash, four samples from the Moreno I outwash, and fourteen samples from three locations on the Moreno II/III outwash terrace. We tested for nuclide inheritance in outwash sediment in two ways. First, we compared outwash and moraine boulder exposure ages from the younger LGM moraine (the outermost and oldest Fenix V moraine limit). If outwash cobble inheritance is low and moraines and terraces have been stable without post-deposition burial or turbation, we expect to find indistinguishable ages that date the timing of that event. Second, we measured the ^{10}Be concentration in an amalgamated sample containing ~50 pebble clasts collected from an undisturbed position at the base of a ~6 m deep gravel quarry within the Moreno II/III outwash terrace (Fig. 5d). To obtain an undisturbed sample, it was necessary to dig a pit 30 cm below the quarry floor. A low ^{10}Be concentration here, well below the original surface, would imply low average nuclide inheritance in the outwash sediment. Finally, we report six additional moraine cobbles from the Moreno I moraines of which 5 were reported by Hein et al. (2009) and one was reported by Kaplan et al. (2005), and four new cobbles (collected in 2006) from the Moreno III moraines. These subangular to subrounded cobbles rarely contain ventifacts, suggesting recent exposure and no surface erosion (Fig. 4d).

3.2 Cosmogenic nuclide analyses

The samples were crushed whole (small cobbles; < 6 cm) or after cutting to an appropriate thickness. In the latter case, samples were cut parallel to the surface, but only when such clasts appeared not to have rotated (e.g., no ventifacts on the underside of the cobble). The crushed rocks were sieved to obtain the 250-710 μm fraction. Cosmogenic ^{10}Be and (in some cases) ^{26}Al were chemically isolated and purified in three separate cosmogenic nuclide laboratories: the University of Edinburgh's Cosmogenic Nuclide Laboratory

(Edinburgh, UK), the Natural Environment Research Council Cosmogenic Isotope Analysis Facility (NERC-CIAF) at the Scottish Universities Environmental Research Centre (SUERC; East Kilbride, UK), and Victoria University of Wellington's Cosmogenic Nuclide Laboratory (New Zealand). Concentrations of ^{10}Be and ^{26}Al were measured at three different Accelerator Mass Spectrometry (AMS) facilities: CologneAMS at the University of Cologne (Cologne, Germany), the SUERC AMS facility (East Kilbride, UK), and the ETH Zurich Laboratory of Ion Beam Physics (Zurich, Switzerland).

3.2.1 University of Edinburgh preparations measured at the University of Cologne

^{10}Be and ^{26}Al was selectively extracted from 2-24 g (average 16 g) of the pure quartz following standard methods (Bierman et al., 2002; Kohl and Nishiizumi, 1992). Process blanks (n = 2xBe; 1xAl) were spiked with 250 µg ^{9}Be carrier (Scharlau Be carrier, 1000 mg/l, density 1.02 g/ml) and 1.5 mg ^{27}Al carrier (Fischer Al carrier, 1000 ppm). Samples were spiked with 250 µg ^{9}Be carrier and up to 1.5 mg ^{27}Al carrier (the latter value varied depending on the native Al-content of the sample). ^{10}Be/^{9}Be and ^{26}Al/^{27}Al measurements are normalised to the standards of Nishiizumi using the revised values reported by Nishiizumi et al. (2007) and Nishiizumi (2004). Blanks range from 3.3-5.0 x 10^{-15} [^{10}Be/^{9}Be] (less than 1% of sample ratios); and 4.8 x 10^{-15} [^{26}Al/^{27}Al] (less than 1% of sample ratios).

3.2.2 NERC-CIAF preparations measured at SUERC

^{10}Be and ^{26}Al were selectively extracted from ~10 g of the pure quartz following standard methods, as described in Darvill et al. (2015b). Process blanks (n = 4xBe; 3xAl) were spiked with ~220 µg ^{9}Be carrier (1082 ppm in-house developed ^{10}Be carrier described as "U Han" in Merchel et al. (2008) and 1.5 mg ^{27}Al carrier (Fischer Al carrier, 985 ppm). Samples were spiked with 230 µg ^{9}Be carrier and up to 1.5 mg ^{27}Al carrier (the latter value varied depending on the native Al-content of the sample). ^{10}Be/^{9}Be and ^{26}Al/^{27}Al measurements are

normalised to the NIST SRM-4325 Be standard material with a revised (Nishiizumi et al., 2007) nominal $^{10}Be/^{9}Be$ of 2.79 x 10^{-11}, and the Purdue Z92-0222 Al standard material with a nominal $^{26}Al/^{27}Al$ of 4.11 x 10^{-11}, which agrees with the Al standard material of Nishiizumi (2004). SUERC ^{10}Be-AMS is insensitive to ^{10}B interference (Xu et al., 2013) and the interferences to ^{26}Al detection are well characterized (Xu et al., 2014). Blanks range from 3.6 – 5.2 x 10^{-15} [$^{10}Be/^{9}Be$] (less than 1% of sample ratios in all but the shielded sample); and 2.8 x 10^{-15} [$^{26}Al/^{27}Al$] (less than 1% of sample ratios).

3.2.3 Victoria University of Wellington preparations measured at ETH Zurich

Pure quartz samples of 12-62 g (37 g average) were extracted from the whole-rock samples (e.g. Kohl and Nishiizumi, 1992). Samples and process blanks (n = 2) were spiked with 300 µg ^{9}Be carrier (GFZ Phenakit Be carrier, 372.5 mg/l). $^{10}Be/^{9}Be$ measurements were performed on the compact 0.5 MV AMS system Tandy (Christl et al., 2013). The measured ratios are normalised to the ETH Zurich in house standard S2007N [nominal $^{10}Be/^{9}Be$ ratio = 28.1 x 10^{-12} (Kubik and Christl, 2010)], which has been calibrated relative to the ^{10}Be AMS standard ICN 01-5-1 with a revised nominal ratio of 2.709 x 10^{-11} (Nishiizumi et al., 2007). The blanks' $^{10}Be/^{9}Be$ ratios (4.4 and 8.2 x 10^{-15}) were less than 1% of the sample ratios for all but the youngest two samples.

3.3 Exposure age calculations

The ^{10}Be and ^{26}Al exposure ages were calculated with the online exposure age calculator formerly known as the CRONUS-Earth online exposure age calculator (version 2.3; Balco et al., 2008) which implements the revised ^{10}Be standardization of Nishiizumi et al. (2007) and the updated global ^{10}Be and ^{26}Al production rate calibration of Borchers et al. (2016). Exposure ages are reported based on the Lal(1991)/Stone(2000) time-dependent scaling model. If instead the ages are calculated using version 2.2 of the exposure age calculator and using the lower, local ^{10}Be production rate for southern Patagonia (Kaplan et al., 2011),

the ages increase by ~3%, which is less than the analytical uncertainties in most cases. For example, an age of 269 ka would increase to 277 ka. The calculator uses sample thickness and density (Table 1) to standardize nuclide concentrations to the rock surface. Topographic shielding was measured but is negligible (scaling factor >0.9998). Shielding by snow, soil, or loess is less problematic here than in more typical mountainous environments due to aridity and persistent winds, therefore no correction is applied. No erosion rate correction is applied even though erosion is sometimes observed (e.g., ventifacts, flattened tops), since the total amount of erosion is generally small (in most cases < 1 cm), and specific to each cobble; therefore, exposure ages are minima. The margins of former ice sheets are areas where strong and persistent katabatic winds create low-pressure zones, which could significantly affect long-term production rates (Staiger et al., 2007). Staiger et al. (2007) modelled this effect and found production rates near ice sheet margins in Patagonia could be ~5% higher than in areas away from ice sheet margins. If the rock samples of the Moreno moraine system had experienced higher production rates throughout their exposure history, then the ages presented could be too old (i.e., the higher production rate would cause exposure ages to decrease by ~5%). However, we do not adjust our cosmogenic ages because the 5% is not constrained by data, and because the exposure history alternated between glacial and interglacial conditions (and stadials and interstadials), and thus presumably pressure fields, for the integrated exposure history of the samples. We acknowledge that if the ice sheet effects during the three glacial maxima (MIS 8, 6 and 2) did increase production rates, our reported ages would be too old, but notably, still within our external uncertainties. Furthermore, boulder erosion and not considering higher production rates during low-pressure periods would have opposing effects on ages. Existing moraine boulder (Douglass et al., 2006; Kaplan et al., 2004; Kaplan et al., 2005) and moraine cobble (Hein et al., 2009) data for the Fenix V and Moreno I-III moraines, and data from the LP valley, have been re-calculated in the same way to yield exposure ages that are directly comparable to the new data.

4. Results

4.1 Geomorphology

Figure 2 shows the limits for the Fenix and Moreno moraines and associated outwash terraces. The Fenix V moraines are largely continuous with 25-30 m relief and side slopes up to 20°. The Moreno moraines are situated ~80 m above the Fenix outwash (Fig. 3). Moraine relief ranges from 20–30 m above the associated outwash terrace (5°–11° side slopes). Fenix and Moreno moraine crests are broad and convex, generally sparsely vegetated with gravel and cobble lag deposits at some locations (Fig. 4). Most moraine boulders are ventifacted, while rounded moraine cobbles are more often not; neither typically exhibit rock varnish. The Moreno I and II moraine limits are largely continuous on the northern and southern side of the valley, but become discontinuous or absent in the centre of the valley, particularly south of Río Deseado. The Moreno III limit is discontinuous throughout and in places is surrounded by younger outwash.

The Fenix and Moreno outwash terraces dip gently southeastward at ~ 0.5° and converge at the entrance to, and above the Río Deseado (Fig. 2). Both terraces are composed of gravels and coarse sands with local concentrations of cobbles and pebbles, which on the Moreno outwash form desert pavements (Fig. 5). These lag deposits are not underlain by fine sediments, which suggests they are not inflationary desert pavements. Vegetation cover is sparse. On the Moreno outwash surface, ventifacts and rock varnish are ubiquitous on surface clasts with some exhibiting ventifacts on all surfaces, suggesting rotation of the clast through time. Soils are thin where measured (10-15 cm) and shallow surface channels (1-3 m) with clear braiding patterns can be observed to grade to moraine limits. Fenix V and Moreno I outwash was sampled at a location where it could be directly traced to the dated moraine. The Moreno I outwash is about 15 m lower than the Moreno II outwash where they join the moraine. The Moreno I outwash is topographically constrained by the higher Moreno II moraines with a scarp separating the two (Fig. 3b). In contrast, it is not possible to unambiguously separate Moreno II and III outwash or directly trace the outwash to specific moraine limits, since the Moreno III moraine is discontinuous

449 and the outwash may have been re-activated when the Moreno II moraines were
450 deposited. For this reason, we do not attempt to separate these outwash units
451 and rather discuss results for the Moreno II/III together. The Moreno II/III
452 outwash was sampled at three locations on both sides of the valley (10 km
453 apart). Sample locations from this study, and previous studies, are shown in
454 Figure 2.
455
456 **4.2 Cosmogenic Nuclide Results**
457
458 The three different wet-chemical and AMS laboratories, and two field parties
459 produced indistinguishable analytical results, which are presented in Tables 1-2
460 and Figs. 2-8. Below, we report previously published but re-calculated moraine
461 boulder (Douglass et al., 2006; Kaplan et al., 2004; Kaplan et al., 2005) and
462 moraine cobble (Hein et al., 2009) exposure ages. ^{10}Be exposure ages are
463 reported throughout the text; the ^{26}Al concentrations are used to explore the
464 potential for burial. Throughout the text, if not stated otherwise, analytical
465 uncertainties are reported at 1σ.
466
467 **4.2.1 Fenix V**
468
469 Sample LBA09-18 is an outwash cobble associated with the Fenix V moraine
470 limit; this sample yields a ^{10}Be exposure age of 24.4±1.1 ka. The moraine
471 boulders from this limit have exposure ages that range between 27.4-18.7 ka, or
472 27.4-23.9 ka excluding the two youngest ages as apparent outliers (Douglass et
473 al., 2006). The outwash cobble falls within the age range of the boulders (Fig.
474 6a). The result suggests that this outwash terrace cobble was no more affected
475 by inheritance or post-depositional burial or turbation than the moraine
476 boulders. The surface exposure ages are consistent with recent OSL dating of
477 Fenix outwash terraces (Smedley et al., 2016), all of which confirms an LGM age
478 for the Fenix moraines using multiple dating techniques.
479
480 **4.2.2 Moreno I-III**
481

Four cobbles from the Moreno I outwash terrace surface yield ^{10}Be exposure ages that range between 261.7-175.9 ka. Fourteen cobbles sampled from three different locations on the Moreno II/III outwash terrace yield ^{10}Be exposure ages that range between 269.0-168.5 ka. The available ^{26}Al/^{10}Be ratios do not indicate prolonged burial of outwash terrace sediment. The outwash cobbles from Moreno I and II/III are indistinguishable in terms of the overall age range and the oldest ages from their surfaces (Fig. 6b). Sample LBA09-10, which came from the bottom of a 6 m-deep gravel quarry, yields a low ^{10}Be concentration of 19000±2000 atoms g^{-1} SiO_2 (equivalent to a surface exposure age of 3.1±0.3 ka). Considering the sample's approximate depth, the concentration is of a magnitude that is consistent with the surface cobble ages; it indicates the average ^{10}Be inheritance in the Moreno outwash sediment is low.

Seven boulders from the Moreno I moraine have ^{10}Be exposure ages that range between 186.8-94.1 ka, excluding one outlier with an age of 37.4 ka (LBA-02-25, which is only ~25 cm high). Five moraine boulders from the Moreno II moraine have ^{10}Be exposure ages that range between 195.6-101.6 ka. Five moraine boulders from the Moreno III moraine have ^{10}Be exposure ages that range between 450.3-123.0 ka. If we consider the two significantly older boulders as outliers, the range is 199.5-123.0 ka. In the latter case, the overall age range is similar for all Moreno moraines (Fig. 6c).

Six moraine cobbles from the Moreno I moraine have ^{10}Be exposure ages that range between 134.0-105.0 ka (Fig. 6c). Four moraine cobbles from the Moreno III moraine, taken in close proximity to the oldest boulder exposure date on Moreno III (sample LBA-02-46; 450±12 ka), yield ^{10}Be exposure ages that range between 109.1-76.5 ka. The youngest sample (LBA06-18) was an amalgamation of 50 pebble clasts from the surface of the moraine. Cobbles from the younger Moreno I moraine are predominantly older than those of the Moreno III moraine, despite two boulders from the latter being much older (*ca.* 450 and 362 ka) than any samples on the former.

5. Discussion

5.1 Glacial Chronology

5.1.1 Nuclide inheritance in outwash

Nuclide inheritance is expected to be low in outwash sediment at LBA. The subrounded cobbles have been transported subglacially >100 km through a warm-based glacier system. Erosion and shielding by the over-riding glacier and meltwater should produce "fresh" rock surfaces containing no inherited nuclides (Hein et al., 2009; Zentmire et al., 1999). Our data confirm this: indistinguishable outwash and moraine boulder exposure ages for Fenix V, and low ^{10}Be concentration in pebbles from deep within the Moreno outwash sediment, indicate that nuclide inheritance can be considered negligible. This finding supports the more thorough study in Hein et al. (2009), which involved a depth profile.

5.1.2 Age of the Moreno outwash terrace

The new cosmogenic nuclide exposure ages are both internally consistent and consistent between multiple cosmogenic nuclide and AMS laboratories. The ages from Moreno II/III and Moreno I outwash terrace cobbles are indistinguishable, suggesting that the outwash was deposited during the same glacial stage (Fig. 6b). However, given the lack of distinction between the Moreno II and III outwash in the field, and two older boulder ages from the moraine itself (*ca.* 450 and 362 ka), taken at face value, the Moreno III could be older (Kaplan et al., 2005). When grouping all Moreno outwash samples together, there is a central peak in the summary plot at ~235 ka, with comparatively fewer older and younger exposure ages (Fig. 6c). The spread in ages and multiple age-distribution peaks from both terraces (Fig. 6b) implies that geomorphological processes are scattering the ^{10}Be concentrations more than the analytical uncertainty. If we assume the Moreno outwash terrace is lowering at a similar rate to the Hatcher outwash terrace in the LP valley (0.53 m Ma^{-1}), then this peak

and the spread of ages can be explained by near-surface cryoturbation and surface deflation through time (Darvill et al., 2015b; Hein et al., 2009; Fig. 7). Cobbles giving the oldest ages remained on the surface as it deflated, while cobbles giving the youngest ages were exhumed from the upper 10-15 cm.

The geologic evidence supports deflation of the terrace surface causing previously buried cobbles to become exposed in the process; some of the youngest samples do not exhibit ventifacts, while the oldest cobbles consistently reveal rock varnish on ventifacts on all sides (Figs. 5e, f). We infer that rock varnish on ventifacts on surface cobbles indicates a longer surface residence time. Because nuclide inheritance is demonstrably low and most geologic processes act to reduce cosmogenic nuclide concentrations, especially outside of the polar regions (Phillips et al., 1990), the oldest ages are considered to best represent the age of the terrace sediment. We acknowledge, however, that even the oldest cobbles could be too young if they too were exhumed, and because no correction for erosion has been applied. In the former case, we consider exhumation unlikely because the oldest surface cobbles are also consistent with the ^{10}Be depth profile data from the Hatcher outwash sediment at LP (Section 5.1.4). In the latter case, even applying a low erosion rate of 0.2 m Ma^{-1} (Douglass et al., 2007) to the oldest outwash cobble would increase the age by 5%, but would yield unrealistically high amounts of total erosion. For example, this rate would imply ~5.5 cm of cobble erosion when less than 1 cm is observed; often the cobbles collected are not much larger than 5-15 cm (Table 2). Thus, we argue that such uncertainty on the exhumation or erosion of the oldest cobbles is minimal and likely within the reported external uncertainties. The oldest cobble ages suggests an age of 269.0±5.2 ka for Moreno II/III, and 261.7±5.1 ka for Moreno I. Given the range of exposure ages for Moreno II/III and I are indistinguishable, we combine the datasets to extract an inferred age for all the Moreno outwash together based on the five samples that make up the oldest peak in the combined summary camel plot (Table 2; Fig. 6c; inset). Based on current knowledge of ^{10}Be production rates and the assumptions made in this paper, we estimate the age of the Moreno outwash to be 265.4±3.5 (1σ external ±29 ka). This is coincident with MIS 8.

5.1.3 Age of the Moreno moraines

The new outwash exposure ages lead us to consider potential implications for the age of the Moreno moraines. With the exception of the two oldest ages from the Moreno III moraine (*ca.* 450 and 362 ka), and excluding moraine cobbles, all existing quantitative data indicate the moraines have a deposition age that broadly coincides with MIS 6; this is a full glacial cycle younger than the age of the outwash terrace (Fig. 6c). This may indeed be the case, considering it is possible that the Moreno moraines were deposited on top of a pre-existing outwash terrace surface. If so, it would imply that the Moreno outwash terrace is a composite feature composed of sediment from two glacial stages; an early advance deposited the terrace material and a second advance produced the younger moraine limits, without adding significant sediment to the outwash plain where we sampled. In this case, perhaps the youngest outwash cobble ages of 169, 174 and 176 ka reflect this younger influx of material (Fig. 6b,c). The idea is also supported by apparent exposure ages from moraine boulders, pedogenic carbonate ages, and by recent OSL dating of sediment accumulations incorporated within the Moreno I, III and Deseado II moraine limits (Smedley et al., 2016).

While the deposition of young moraines on old outwash is conceivable, this view is not compatible with the age of the Moreno I outwash terrace. Specifically, the Moreno I outwash terrace, with an age of 260-270 ka, is situated in a morphostratigraphically younger position in the landscape, being inboard of, and topographically lower than the Moreno II/III moraine limits (Fig. 3b). In other words, the older Moreno I outwash terrace is bounded by two apparently younger moraine limits. Given the evidence for warm-based conditions, we suggest that the overriding glacier that deposited the Moreno II/III moraines would have destroyed the pre-existing outwash terrace. Thus, it seems unlikely that the Moreno II/III moraines could be younger than 260-270 ka. On the other hand, the less extensive Moreno I moraine, hypothetically, could be younger since it was deposited up-ice of the dated terrace. The same logic applies to the

entire Moreno system, which is situated inboard of – and topographically lower than – the entire Deseado system (Fig. 3a). Smedley et al. (2016) inferred a MIS 6 age for the more extensive Deseado II outwash system on the basis of an OSL age of 123±18 ka. We consider it unlikely that the moraines themselves could be so young because the overriding glacier that deposited the more extensive Deseado moraines would have destroyed the older, but less extensive Moreno II/III outwash terrace, which has an age of 260-270 ka. Thus, we suggest the Deseado moraines must be at least MIS 8 in age, and most likely they pre-date MIS 8 (cf. Kaplan et al., 2005). Likewise, the Moreno III moraine could also pre-date MIS 8 since the dated outwash cannot be unambiguously linked to the moraine and because some boulders from this moraine have older ages.

We favour a scenario where the Moreno moraine and outwash terrace system represents a single glaciation, but factors affecting the geochronological data have led to the measured age-discrepancy. Given the potential age of the moraine systems, we suggest rock surface erosion and exhumation of moraine boulders and cobbles may help to explain the comparatively young surface exposure ages. At least for Moreno I and II, the oldest moraine boulders suggest a deposition age of *ca.* 188 ka, and 195 ka, respectively, which is about 75-80 ka younger than the oldest outwash cobbles. The multiple peaks in the moraine boulder age distribution (Fig. 6c) are suggestive of geomorphological processes that may be affecting the boulder exposure ages.

5.1.3.1 Erosion and exhumation of moraine samples

Evidence of ventifacts on boulders suggests that rock surface erosion may play a role in the wide scatter and young exposure ages due to the physical loss of cosmogenic nuclides from the rock surface (Kaplan et al., 2005). The boulders protrude above the moraine surface where they are exposed to debris carried by wind. We argue that such erosion occurs during glacial maxima when outwash plains are actively producing debris that can be entrained by winds (Hein et al., 2009; Sugden et al., 2009). This episodic style of erosion is difficult to correct for, since the magnitude of total erosion cannot be visually assessed on boulders

646 and because applied erosion rates are long-term averages. Interestingly,
647 however, applying a maximum erosion rate (1.4 m Ma^{-1}; Kaplan et al., 2005) to
648 the oldest boulder (LBA-02-48; Moreno III) increases its age from 200 ka to
649 about 250 ka.
650
651 While erosion clearly plays a role in reducing apparent exposure ages from
652 moraine boulders, there is geomorphological and isotopic evidence to suggest
653 that exhumation is a primary control. Several upstanding (50-200 cm) moraine
654 boulders exhibit deep flutings and ventifacts on their top surfaces, but these
655 erosional features are less developed on their lower surfaces nearest the ground
656 (Fig. 4a,b). Moreover, unlike outwash cobbles, moraine cobbles of comparable
657 size and lithology are rarely ventifacted, suggesting exposure after the most
658 recent pulse of aeolian erosion (Fig. 4d). Aeolian erosion is normally limited to
659 within ~50 cm of the ground surface (Bagnold, 1941), suggesting the well-
660 developed erosional features on the tops of boulders were formed when the
661 boulder surface was closer to the ground. Scatter in the age-distribution of
662 moraine boulders approximately follows the profile predicted by models of
663 moraine degradation, as opposed to the profiles predicted for inheritance or
664 measurement error (Applegate et al., 2012).
665
666 The smaller moraine cobbles yield exposure ages that are consistently young,
667 comparatively less scattered and without co-isotopic evidence for post-
668 depositional burial. Hein et al. (2009) interpreted the low concentrations as a
669 degradation signal, using the lowest concentrations in Moreno I moraine cobbles
670 to infer continuous degradation rates of 7.6 m Ma^{-1} or 6.1 m Ma^{-1} for a moraine
671 with an age of 260 ka or 170 ka, respectively; these rates equate to about 200-
672 105 cm of surface lowering. Using the same approach for the Moreno III moraine
673 cobble data yields rates of 8.9 m Ma^{-1} or 7.1 m Ma^{-1}, which equates to about 230-
674 120 cm of surface lowering. The rates derived here are indistinguishable to
675 those determined for the older Telken moraines in the same valley, at 7 m Ma^{-1}
676 (Ackert and Mukhopadhyay, 2005). This simple sensitivity test suggests the
677 Moreno moraines could have lowered by 230-100 cm since deposition. Most
678 sampled boulders were smaller than 100 cm, but there is no clear age-

679 dependence on boulder height (Table 2), although short moraine boulders may
680 be more likely to give younger ages than the population mean (e.g., LBA-02-25
681 and LBA-01-66)(Heyman et al., 2016). While we acknowledge that moraine
682 degradation rates are unlikely to have been continuous or spatially uniform, the
683 sensitivity results and our geomorphological observations suggest moraine
684 degradation may be a key process to explain the young and scattered moraine
685 boulder exposure ages. It may be that moraine degradation, similar to rock
686 surface erosion, accelerates during glacial periods due to increased meltwater
687 erosion and changes in climate that favour increases in soil moisture,
688 cryoturbation and wind (Kaplan et al., 2007). Katabatic winds off the large
689 Patagonian Ice Sheet when it existed (Fig. 9) may have led to relatively brief
690 periods of more intense erosion. Such changes in soil moisture and
691 cryoturbation may also help to explain the pedogenic carbonate ages, and the
692 youngest peak in outwash cobble ages. The processes inferred, however, do not
693 help to explain the similarly young OSL ages from the same moraines, since these
694 dates derive from material incorporated within the moraine limits. The reason
695 for this discrepancy is unclear and is an avenue for further research.
696
697 **5.1.4 Correlation to Lago Pueyrredón**
698
699 Exposure ages reveal a striking consistency between both the Fenix and Moreno
700 moraine systems, and the Río Blanco and Hatcher moraine systems in the LBA
701 and LP valleys, respectively (Fig. 8). On older moraines, the exposure age
702 consistency depends on the type of sample: the age ranges for moraine boulders
703 and outwash terrace cobbles yield consistently differing ages within each valley,
704 and the moraine cobbles are generally the youngest exposure ages. This
705 consistency suggests that the processes responsible for producing the age
706 distributions are likely to be the same in both valleys. A depth-profile through
707 Hatcher outwash sediments confirms the interpreted age of the Hatcher (and
708 Moreno) outwash terraces as coincident with MIS 8 (Hein et al., 2009). The
709 indistinguishable ages for the two moraine systems validate the
710 morphostratigraphy. The Fenix moraines are age-equivalent to the Río Blanco
711 moraines, and the Moreno moraines are age-equivalent to the Hatcher moraines.

We highlight that this result is independent of systematic changes in, for example, production rates, scaling models or pressure fields, which would affect the absolute age of the deposits, but not the fact that the two glaciations in both valleys are the same. The Fenix and Río Blanco moraines represent a glaciation during MIS 2, while the Moreno and Hatcher systems represent a glaciation during MIS 8.

5.2 Wider implications

5.2.1 Implications for exposure dating old moraine systems

Our results reinforce that outwash terraces can be effective targets for exposure dating to constrain ice sheet history (Darvill et al., 2015b; Hein et al., 2011; Hein et al., 2009). In Patagonia, environmental conditions provide a good setting for using outwash cobbles to date glaciations, given aridity and persistent winds limit the opportunity for shielding by materials such as snow, soil or loess, and ensure generally low erosion (or inflation) rates for the terrace surface. In mountainous environments, these factors may play a significant role inhibiting the buildup of cosmogenic nuclides in outwash sediment and invalidate the approach. The generally thin soils in the region limit turbation to the upper few cm of the deposit, minimizing the exhumation depth and scatter in surface cobble ages. Furthermore, the local geomorphology suggests outwash terraces were abandoned post deposition and were not subsequently reactivated. Shallow channels several meters deep survive on Moreno and Deseado outwash that are several hundred thousand years old. The approach is advantageous for reconstructing the Middle to Late Quaternary climate evolution in Patagonia because outwash plains of this age are more commonly preserved than moraine records. Therefore, dating these surfaces has the potential to fill an important gap in the Quaternary glacial record that could not be obtained using the moraine record alone; in some cases dating the outwash may be the only effective way to constrain the age of associated moraine limits. The surface cobble approach, ideally in combination with depth-profiles, is demonstrably

744 effective in Patagonia but may also work well in similar environments elsewhere
745 where warm-based glaciers produce distinct outwash plains.
746
747 This study adds to a growing body of data that demonstrate the challenge of
748 dating old moraine records using surface exposure methods (Balco, 2011; Darvill
749 et al., 2015b; Hein et al., 2009; Heyman et al., 2011). Putkonen and Swanson
750 (2003) recommended sampling at least six to seven boulders from old and tall
751 moraines to obtain a boulder age at ≥ 90% of the moraine age (95% confidence).
752 However, in central Patagonia, twenty moraine boulders from the Moreno and
753 Hatcher moraines still appear to have underestimated the timing of glaciation by
754 70-100 ka (i.e., a full glacial cycle). This suggests that exhumation and erosion
755 was sufficient to invalidate all sampled boulders. In Patagonia, the difficulty
756 includes cases where it can be shown that apparent old 'outliers' in an age
757 population date closely the glacial advance (Hein et al., 2011), and cases where
758 such outliers can be shown to contain inherited nuclides, as in the case of a study
759 of erratic boulder trains in Tierra del Fuego (Darvill et al., 2015a; 2015b).
760
761 Our findings beg the question, for how long does boulder moraine (or cobble
762 outwash) dating afford accurate ages for old (pre-LGM) landforms? On the
763 Pukaki moraines in New Zealand, 36 boulders give consistent ^{10}Be ages (within
764 analytical uncertainties alone) of ~70-60 ka (mean is 65.1±2.7 ka), indicating a
765 significant MIS 4 advance (Schaefer et al., 2015). The consistency of the ages and
766 general lack of geomorphological evidence for exhumation suggests that the
767 boulders provide a robust age for the moraine. Thus, moraine boulders can be
768 used to date pre-LGM moraines, but perhaps typically only within the last glacial
769 cycle. The reliability will inevitably depend on the specific depositional and post-
770 depositional environment, especially prior to the last glacial cycle or MIS 5.
771
772 Finally, the application of OSL dating to sediments incorporated within glacial
773 moraines and outwash terraces offers an opportunity to gain additional insight
774 into glacial evolution. Smedley et al. (2016) were able to identify an older glacial
775 advance from sediment accumulations situated within a younger outwash
776 terrace beneath the Fenix V moraine. Thus, the OSL technique can help to fill an

important gap in the glacial history, including places where no moraines or outwash terraces are preserved.

5.2.2 Mid-Pleistocene glaciations

The chronology gives evidence for a regionally significant mountain glaciation in central Patagonia during MIS 8 and MIS 2 (Fig. 9). The maximum outwash cobble ages coincide with the peak in northern hemisphere ice volume as inferred from $\delta^{18}O$ isotopic values in benthic foraminifera (Lisiecki and Raymo, 2005). The timing also coincides with the coldest Antarctic temperatures and peaks in dust and winter sea ice extent as inferred from proxies in Antarctic ice cores (EPICA, 2004; Lambert et al., 2008; Wolff et al., 2006). A Patagonian origin of mineral aerosols has been inferred based on Sr, Nd and Pb isotopic composition (Basile et al., 1997; Delmonte et al., 2004; Sugden et al., 2009), and the dust peaks have been linked to glacial maxima in a source area of southern Patagonia (Sugden et al., 2009). Thus the expansion of central Patagonian glaciers during MIS 8 and 2 is consistent with major dust peaks at this time. The Moreno and Hatcher outwash terraces probably began forming (and producing dust) earlier in the glacial stage, perhaps as indicated by the slightly older outwash ages in the LP valley, but stabilized near its end, if our exposure ages are taken at face value. The advance of the Patagonian Ice Sheet at the peak of MIS 8 and 2, and its retreat during Terminations III and I, are important in demonstrating that Quaternary glacial maxima are indeed broadly global in nature. Despite out-of-phase insolation intensity, the southern mountain glaciers experienced glacial maxima and retreat at approximately the same time as the northern hemisphere ice sheets, supporting the orbital forcing model for the overall timing of Quaternary glaciations (Denton and Hughes, 1983; Hays et al., 1976; Imbrie et al., 1993).

In contrast to other parts of Patagonia and New Zealand, we find no direct cosmogenic nuclide evidence at LBA or LP for glacial advances during MIS 6, 4 or 3, although we recognize the Moreno I moraine (or parts of it) possibly could date to MIS 6. This implies that glacial advances at these times were similar to or

less extensive than those during MIS 2 and/or their records were destroyed or remobilized by subsequent glacial activity. The latter may have resulted from constrained meltwater flow as a consequence of the over-deepened nature of the valleys forcing meltwater between the glacier and the Moreno I scarp and into the Río Deseado (Hein et al., 2009; Kaplan et al., 2005). The fact that so many boulder (and cobble) exposure ages at LBA and LP concentrate around MIS 6 could indicate that the conditions that facilitate exhumation and exposure of such clasts were particularly intense during this period, especially on Moreno I (Fig. 4c) and II crests that could have been so close to the front of the ice margin. While Antarctic temperatures were equally cold as in later glacial stages, MIS 8 was not a significant ice age in terms of global ice volume, particularly in comparison to MIS 6 and 2 (Fig. 9; Lisiecki and Raymo, 2005), yet it resulted in the more extensive glacial advance in central Patagonia. At present, there is too little data available from other parts of Patagonia to demonstrate whether this advance was equally extensive across the former ice sheet, or whether different parts of the ice sheet responded in different ways (e.g., Rabassa et al., 2011).

The cause of the large MIS 8 advance compared to more recent glacial stages is unclear. One possibility is that the advance resulted from a difference in climatic conditions. Southern Hemisphere summer insolation is unlikely to have been a major factor given it was not significantly weaker during MIS 8. The location of the southern westerly winds and oceanic currents have also been proposed as a significant driving factor in the timing and latitudinal variability of glacial advances in Patagonia (Darvill et al., 2016; Herman and Brandon, 2015; Lamy et al., 2004). Reduced, possibly prolonged, offshore sea surface temperatures and/or increased precipitation and reduced temperature due to a strengthening and/or equatorward displacement of the moisture-bearing westerly winds could have caused an extensive glacial advance during MIS 8 in central Patagonia that differed from the global trend. However, current proxy records for changes in temperature and precipitation at this time are inadequate to support such a hypothesis.

Another possibility is that Patagonian Ice Sheet elevation and extent are related to the duration of a glacial period. Specifically, the length of cooling in Antarctica may exert an influence on climate and the buildup of ice in the southern mid-latitudes. Given the Moreno outwash terrace dates to near the end of MIS 8, particularly when considering the possible effect of a lower pressure field during glacial times (section 3.3), it may indicate the time of maximum ice extent. The overall temperature decrease in Antarctica was similar to other glacial stages, but there are subtle differences in the pattern of cooling (Fig. 9). For example, the decline in Antarctic temperature from MIS 9 and into MIS 8 appears relatively continuous in comparison to the decline from MIS 7 and into MIS 6. The latter was interrupted by a significant warming phase during the interglacial MIS 7a and 7c, which should have halted or reversed the buildup of the Patagonian Ice Sheet. Thus, maximum ice elevation in Patagonia may only be achieved after a long and continuous phase of cooling in the southern hemisphere, as in MIS 8 and MIS 2.

Also, a MIS 6 and MIS 2 advance in this region may have been less extensive than MIS 8 due to a non-climatic process. One distinct possibility is a feedback between glacial erosion and ice extent. If the MIS 8 advance caused over-deepening of the valley floor, then subsequent glacial activity may have been restricted in a manner that was decoupled from climatic cooling. This mechanism has been proposed to explain the pattern of nested Quaternary glacial sequences found throughout Patagonia (Anderson et al., 2012; Kaplan et al., 2009). However, given that MIS 8 produced lower global ice volume than preceding stages (MIS 10 and 12), this would either demand that MIS 8 was anomalously strong in Patagonia or that excessive valley erosion was not linked to climate.

Our finding of anomalous glacial activity during MIS 8 is an incentive to collect geographically-dispersed and longer records of Quaternary palaeoenvironmental change from the region. The over-deepened valleys of central Patagonia are unique in preserving evidence for several Quaternary glacial advances. On the other hand, the over-deepenings could result in aspects of glacial records that are decoupled from climate, specifically the pattern of landforms that are

875 preserved from different glaciations. Increasing the latitudinal range of glacial
876 chronologies from sites without over-deepenings may prove useful in providing
877 insight on the forcing of Quaternary glaciations in the southern hemisphere.
878
879 **6. CONCLUSIONS**
880
881 • ^{10}Be exposure ages from 18 outwash cobbles yield exposure ages of 174-
882 269 ka. The five oldest outwash cobbles indicate the Moreno outwash
883 terrace in the Lago Buenos Aires valley was deposited at *ca.* 260-270 ka,
884 with a mean of 265.4±3.5 (1σ external ±29 ka). The outwash was
885 deposited at the same time as the Hatcher outwash terrace in the
886 neighbouring Lago Pueyrredón valley.
887 • The new chronology validates the morphostratigraphic model; the Fenix
888 and Moreno systems are age-equivalent to the Río Blanco and Hatcher
889 systems in the Lago Buenos Aires and Lago Pueyrredón valleys,
890 respectively. The data indicate regionally significant glacial advances
891 occurred in central Patagonia during MIS 8 and MIS 2.
892 • The geomorphology and the new chronology suggest the Moreno
893 moraines were deposited at the same time as the dated outwash terraces
894 that they are specifically linked to. Based on three different approaches to
895 exposure dating of glacial limits, we propose that erosion and exhumation
896 of moraine boulders resulted in surface exposure ages that underestimate
897 the deposition age by 70-100 ka, at least for Moreno I and II (and possibly
898 Moreno III).
899 • The advance of the Patagonian Ice Sheet at the peak of MIS 8 and MIS 2,
900 and its retreat during Termination III and I, demonstrate a correlated
901 response between southern hemisphere mountain glaciers and northern
902 hemisphere ice sheets, suggesting broad interhemispheric synchronicity
903 of ice age maxima during the mid to late Pleistocene. The cause of the
904 large MIS 8 advance in central Patagonia during a comparatively minor
905 global ice age is unclear, and is an avenue for future research.
906
907

ACKNOWLEDGEMENTS

We thank the UK Natural Environment Research Council's Cosmogenic Isotope Analysis Facility (NERC-CIAF) for funded sample analyses conducted in their laboratory (Project 9079.1009). We thank Christoph Schnabel for help processing samples at the CIAF and Carly Peltier for discussion. MRK acknowledges funding in part from NSF-BCS 12-63474. CMD conducted this research while in receipt of a UK NERC Ph.D. studentship at Durham University (NE/j500215/1). This is LDEO contribution # XXXX.

Figure captions.

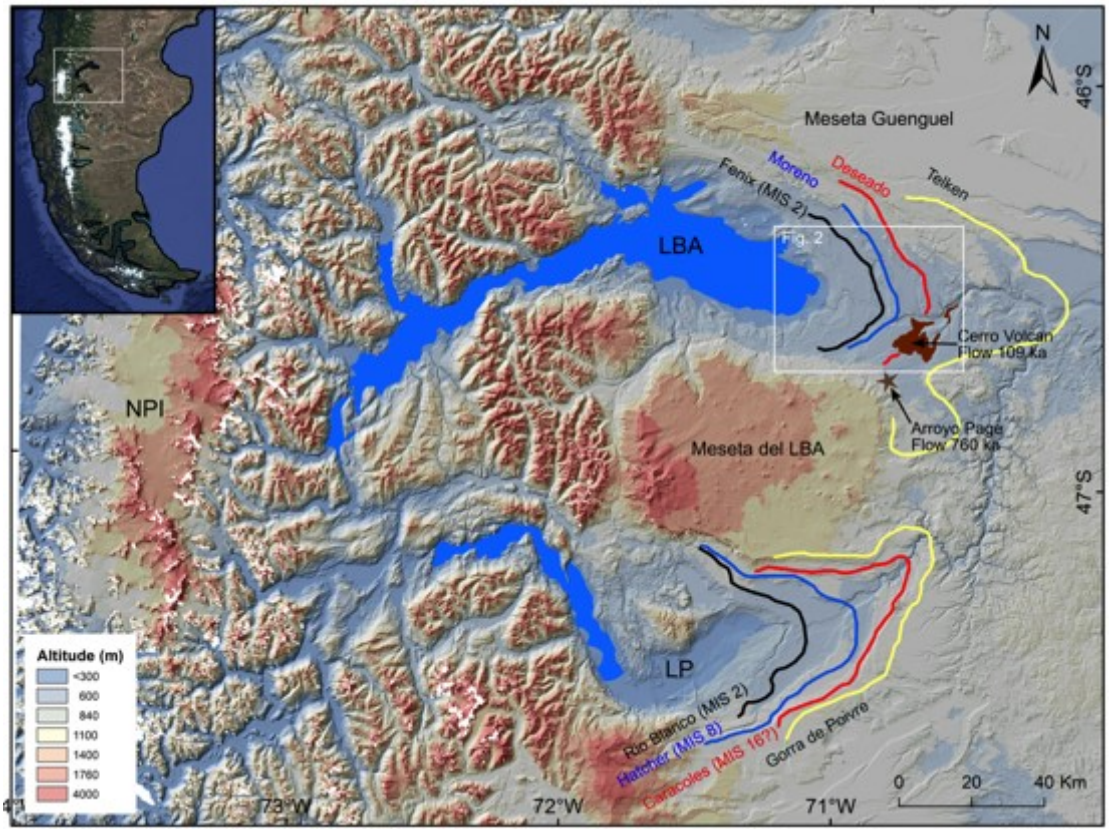

Figure 1. The figure shows the location of the field site in central Patagonia and the present-day North Patagonian Icefield (NPI). The over-deepened Lago Pueyrredón (LP) and Lago Buenos Aires (LBA) valleys were conduits for major outlet glaciers of the Patagonian Ice Sheet. The figure shows the approximate position of the key moraine limits preserved in each valley, their approximate age and Marine Isotope Stage (MIS), and other geographical information. The present study aims to validate the morphostratigraphic relationships for the penultimate Moreno/Hatcher moraine systems. The figure is derived from Shuttle Radar Topography Mission (SRTM) 30 m digital elevation model (DEM). The inset shows the location in southern South America.

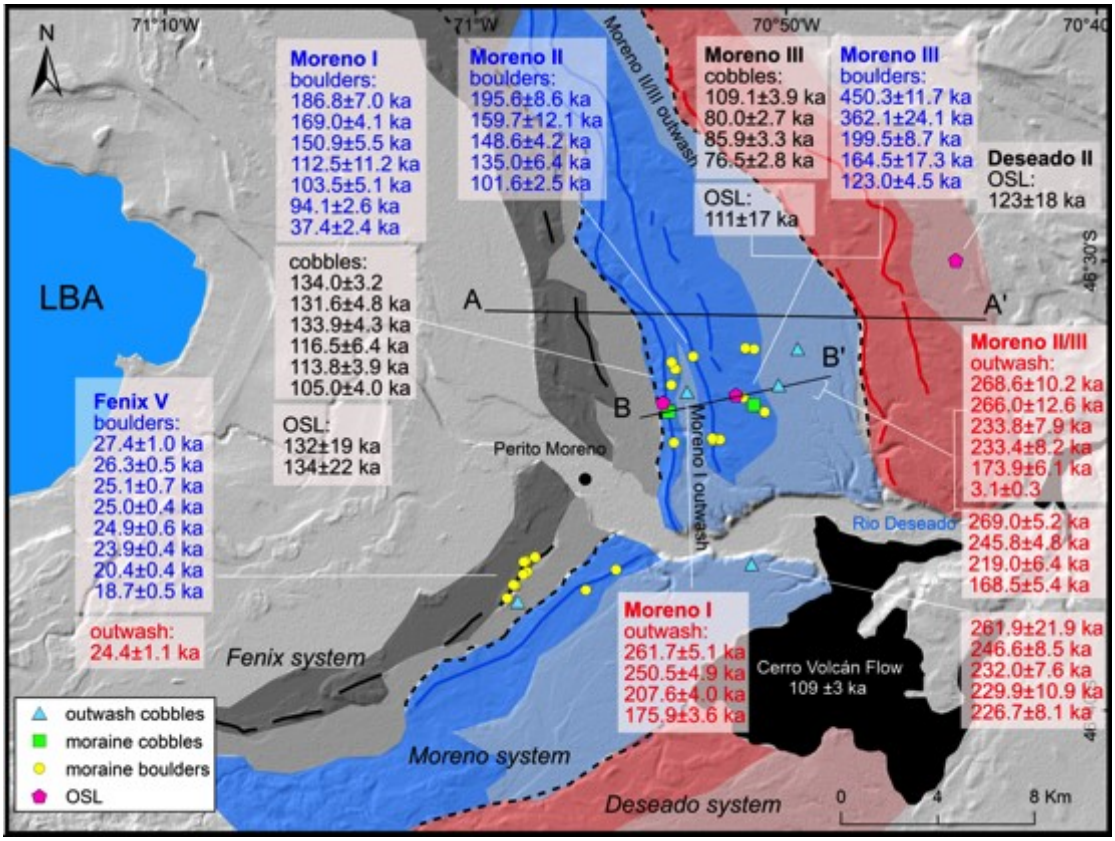

Figure 2. The Lago Buenos Aires field site and sample locations. The figure shows the key moraine systems with darker shades corresponding to areas dominated by moraine-till, and lighter shading to areas dominated by outwash sediments. The sample locations, ages and analytical uncertainties for each sample type are shown (see Tables 1 and 2 for full sample details). The A-A' line and B-B' line are the profiles shown in Figure 3. All previously reported exposure ages have been re-calculated to be consistent with the present study (see Section 3.3). The moraine boulder exposure ages from the Fenix moraines are from Douglass et al. (2006) and Kaplan et al. (2004), and for the Moreno moraines, Kaplan et al. (2005). Moraine cobbles exposure ages from Moreno I are from Hein et al. (2009), and from Moreno II/III are from this study, OSL ages are from Smedley et al. (2016), and the $^{40}Ar/^{39}Ar$ age of the Cerro Volcan lava flow is from Singer et al. (2004). All outwash ages are from the present study. The figure is derived from a hill-shaded Shuttle Radar Topography Mission 30 m digital elevation model.

955

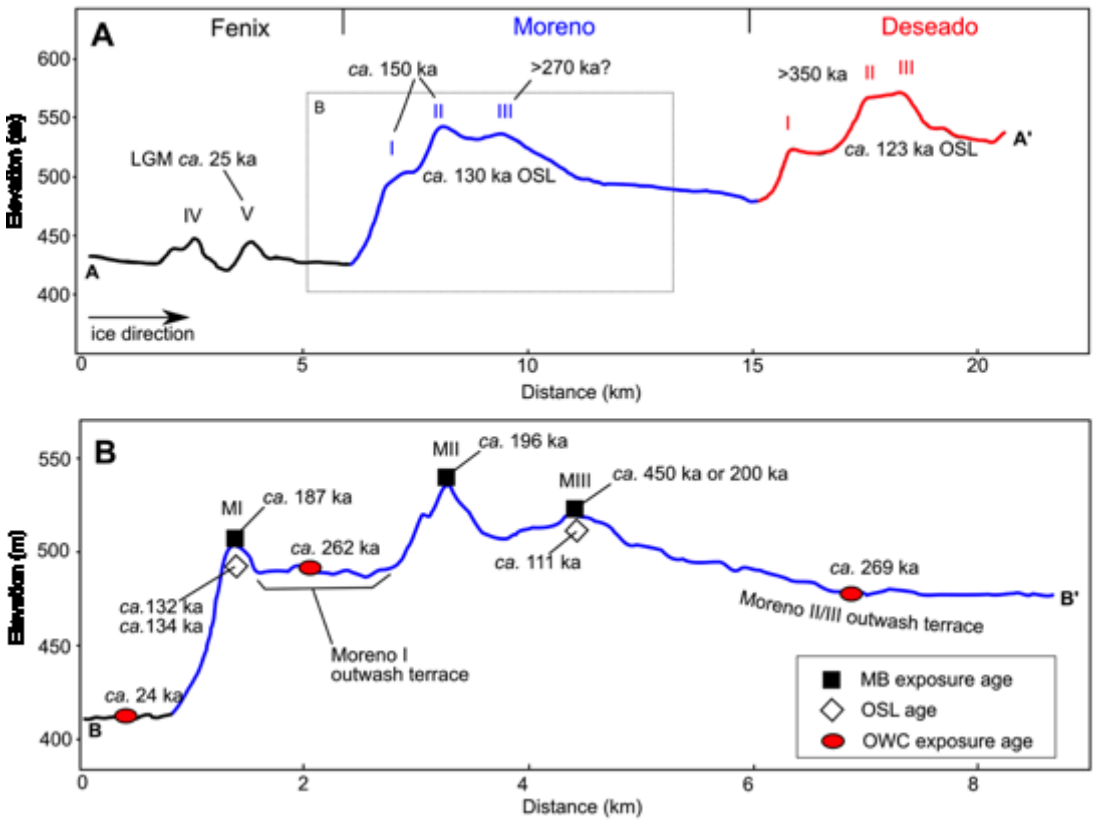

Figure 3. Surface profiles across the moraine sequences at Lago Buenos Aires. A) Profile showing surface elevation change along the A-A' line in Figure 2. The figure shows the key moraine sequences and individual moraine limits (numbered). The approximate ages for the landforms are shown based on existing (not re-calculated) cosmogenic nuclide data from moraine boulders (Douglass et al., 2006; Kaplan et al., 2005) and OSL data (Smedley et al., 2016). The figure illustrates the distinct scarps that separate the different glacial sequences. B) The profile shows surface elevation change along the B-B' line in Figure 2, which cuts across the Moreno system. The figure shows the three Moreno moraine limits (MI-III) and recalculated exposure ages for the oldest moraine boulders (MB) from each (for Moreno III we also include the oldest of two apparent 'outliers'), the OSL ages, and the oldest outwash exposure ages (OWC) from this study. Uncertainties are not shown but are available in Table 2. The figure illustrates how the older Moreno I outwash terrace is situated inboard of and topographically lower than the apparently younger Moreno II/III moraines. We argue the Moreno II/III moraines could not be younger than *ca.* 260 ka, the age of the Moreno I outwash terrace. Likewise, agreeing with prior studies (Kaplan et al., 2005), we argue the Deseado moraine system cannot be

younger than *ca.* 260 ka. In both figures, former ice direction is left to right. The profiles were extracted from a Shuttle Radar Topography Mission 30m digital elevation model.

978

979

980 **Figure 4.** Photographs of Moreno moraine surfaces and typical moraine
981 samples. A) Photo of a moraine boulder (~60 cm high) showing evidence of
982 aeolian erosion and exhumation. Fluting and ventifacts decrease toward the
983 moraine surface, suggesting some degree of exhumation. The sample location of
984 Moreno I outwash is visible. B) Photo of the oldest moraine boulder on Moreno
985 III (Table 2), showing a similar pattern of aeolian erosion and exhumation. The
986 figure also shows the shrub vegetation that is common on Moreno moraines. C)
987 The Moreno I moraine crest at the location where the moraine cobbles were
988 sampled just above the Fenix outwash terrace. The crest is broad, largely
989 vegetated but with occasional gravel-cobble lag deposits such as this. D) A
990 typical moraine cobble showing little evidence of aeolian erosion or rock varnish.
991

992

993 **Figure 5.** Photographs of Moreno outwash terrace surfaces and typical outwash
994 cobble samples. A) Desert pavements are well established on many parts of the
995 Moreno outwash terrace. Rock varnish and ventifacts on surface cobbles are
996 ubiquitous. B) The Moreno II/III outwash terrace surface showing little
997 vegetation; this is common for all Moreno outwash terraces. The sample shown
998 is the same as in panel C. C) This photograph shows rock varnish on ventifacts,
999 on the underside of a surface cobble. This suggests rotation of the surface clast
1000 through time, and a long surface residence. D) Photo taken within a ~6 m deep
1001 gravel quarry, where we obtained an amalgamated sample containing 50 quartz
1002 pebbles to evaluate whether outwash materials contain inherited cosmogenic
1003 nuclides. The samples were collected in a pit that was dug a further 30 cm below
1004 the base of the gravel quarry where the clasts were undisturbed. E) Rock varnish

and ventifacts are not well developed on this sample from the Moreno II/III outwash, in agreement with its relatively young age. This may indicate recent exhumation from depth. F) One of the oldest outwash cobbles showing rock varnish well developed on ventifacts. We suggest cobbles like these survived on the surface as the terrace deflated downward.

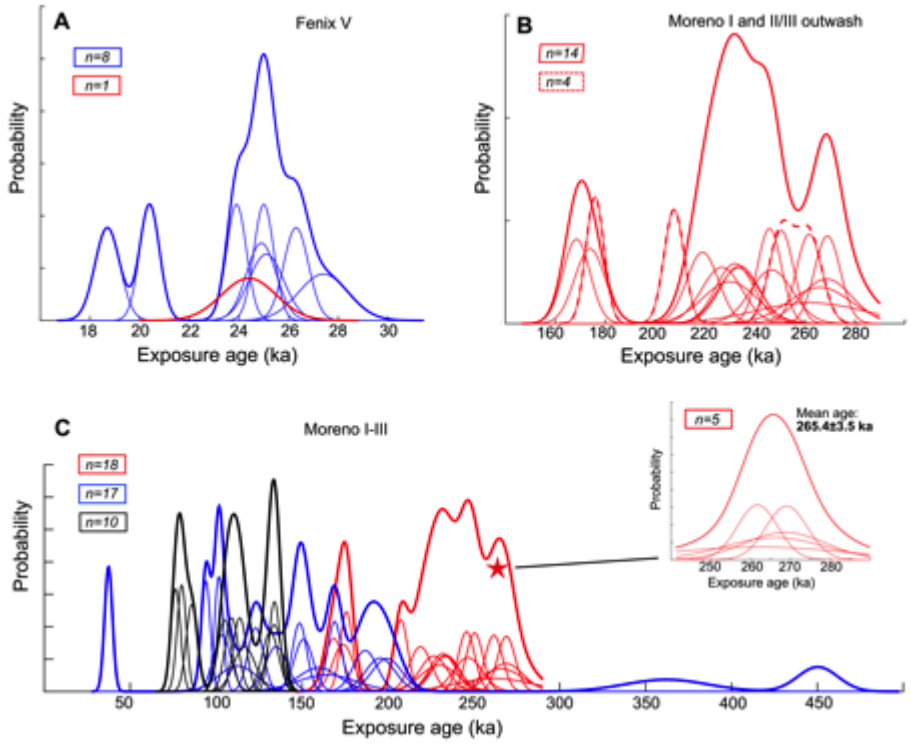

Figure 6. Camel plots showing ^{10}Be exposure ages and internal uncertainties for different sample types on the Fenix V and Moreno I-III moraine systems (n= the number of samples making up each group of data). Note the area beneath each individual Gaussian curve is the same, thus their height is inversely proportional to the measurement uncertainty. A) Plot showing all of the sampled Fenix V moraine boulders (blue) and the single outwash cobble (red). The single outwash cobble gives an LGM age that is indistinguishable from the moraine boulder ages; this is argued to suggest moraines and outwash sediment are deposited with few inherited nuclides. Douglass et al., (2006) did infer the two youngest ages were outliers. B) Plot showing the samples from Moreno I outwash (dashed lines) and the Moreno II/III outwash (solid lines). Both terrace surfaces have a similar age range, suggesting they were deposited at approximately the same time. The multiple peaks are suggestive of geomorphological processes affecting the exposure age results. C) Plot showing all Moreno outwash cobbles (red), moraine boulders (blue) and moraine cobbles (black) together. The figure illustrates how the exposure age is dependent on the nature of the sample and the sample location, including which moraine (Moreno III is stratigraphically the oldest). In general, outwash cobbles are consistently

older than moraine boulders while moraine cobbles are the youngest. We argue episodic moraine degradation and rock surface erosion is responsible for the consistently younger moraine exposure ages. The inset shows a camel plot of the five oldest outwash cobble exposure ages making up the oldest peak in the combined camel plot (red star); we take the mean and standard deviation as our preferred age interpretation for the Moreno moraine system.

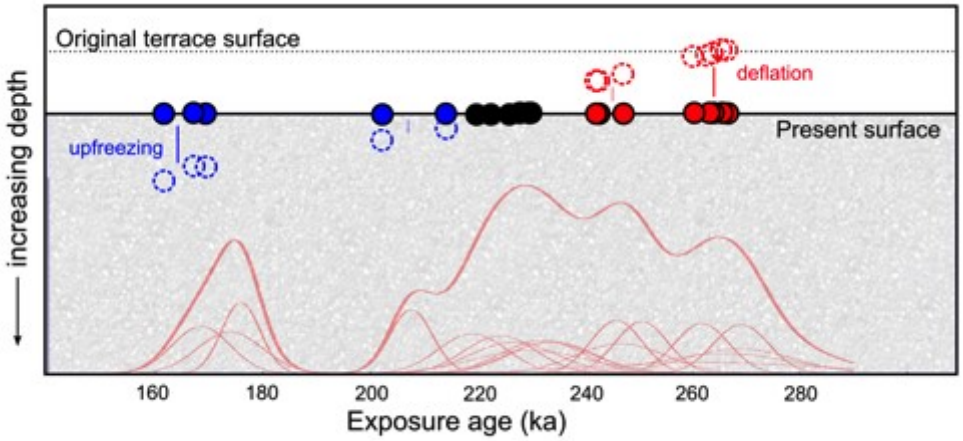

Figure 7. A cartoon depicting our explanation of the observed scatter in the outwash cobble exposure ages viewed as a cross-section through the terrace. The y-axis displays depth within the terrace sediment, while the x-axis shows age. Also shown are the camel plots and exposure ages of the measured cobbles (solid circles) collected from the present-day surface (solid horizontal line). Thin lines are individual ages and thick lines the summed probability. The original depositional surface (dotted line) has deflated through time to the present day position. The bulk of outwash cobbles have remained *in situ* (black), which corresponds with the peak in the camel plot. However, several surface cobbles remained on the surface or became exposed as the surface lowered (red), while others have been brought to the surface through cryoturbation (blue). We infer terrace erosion rates of ~0.5 m Ma^{-1} (Hein et al., 2009) equating to about 14 cm of surface lowering. Measurements of soil depth are 10-15 cm, suggesting upfreezing is likely limited to the upper surface.

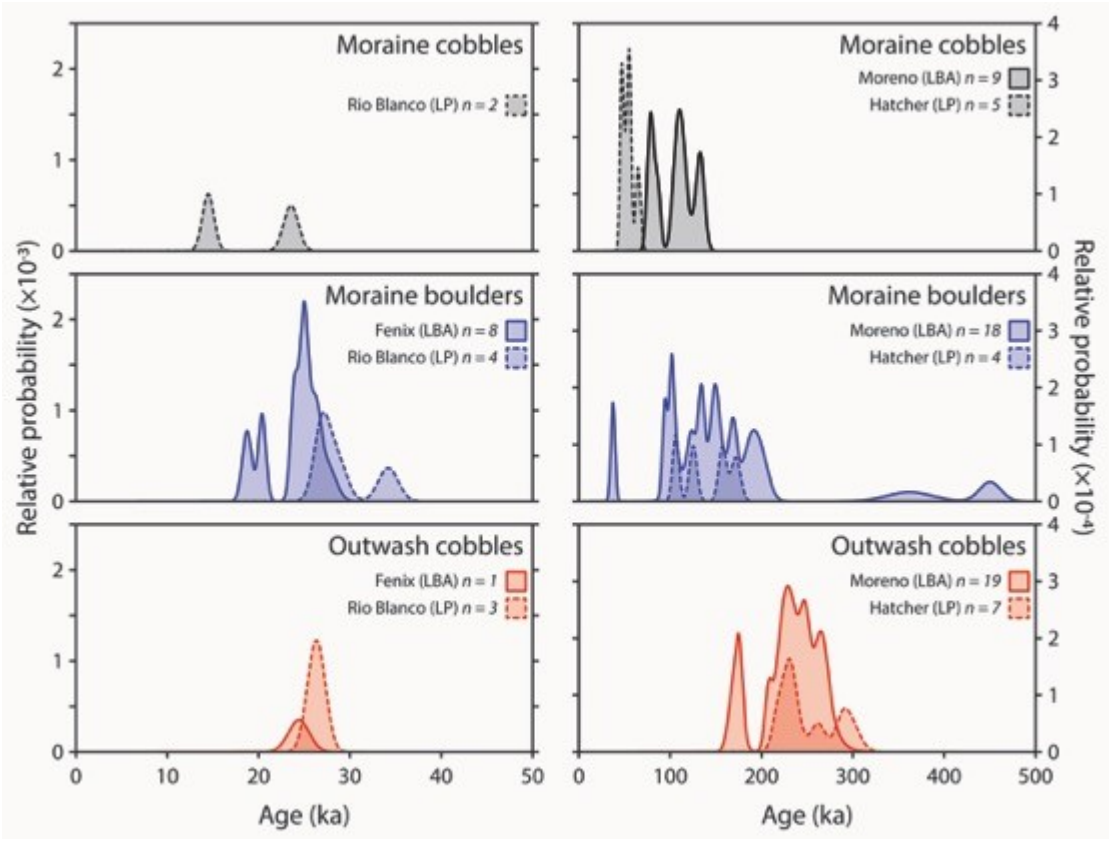

Figure 8. Comparison of exposure ages between the Lago Buenos Aires (LBA; solid lines) and Lago Pueyrredón (LP; dashed lines) valleys. The camel plot shows all exposure ages (including outliers) obtained from outwash cobbles (red), moraine boulders (blue) and moraine cobbles (black) for the Moreno and Hatcher systems (right), and the Fenix and Río Blanco systems (left). We note that boulders from Moreno III (which include the two oldest) are clumped together with boulders from Moreno I and II; this might not be appropriate since the Moreno III moraine may be older. Exposure ages are indistinguishable between the two valleys and suggest an LGM age for the Fenix/Río Blanco systems. For the Moreno and Hatcher systems, moraine boulders and outwash cobbles yield consistently differing ages within each valley. We infer that moraine cobbles reflect moraine degradation, which is not spatially uniform given that moraine cobble exposure ages are slightly younger in the LP valley. The data for the LBA valley are in Tables 1-2, while the data from the LP valley are from Hein et al. (2009).

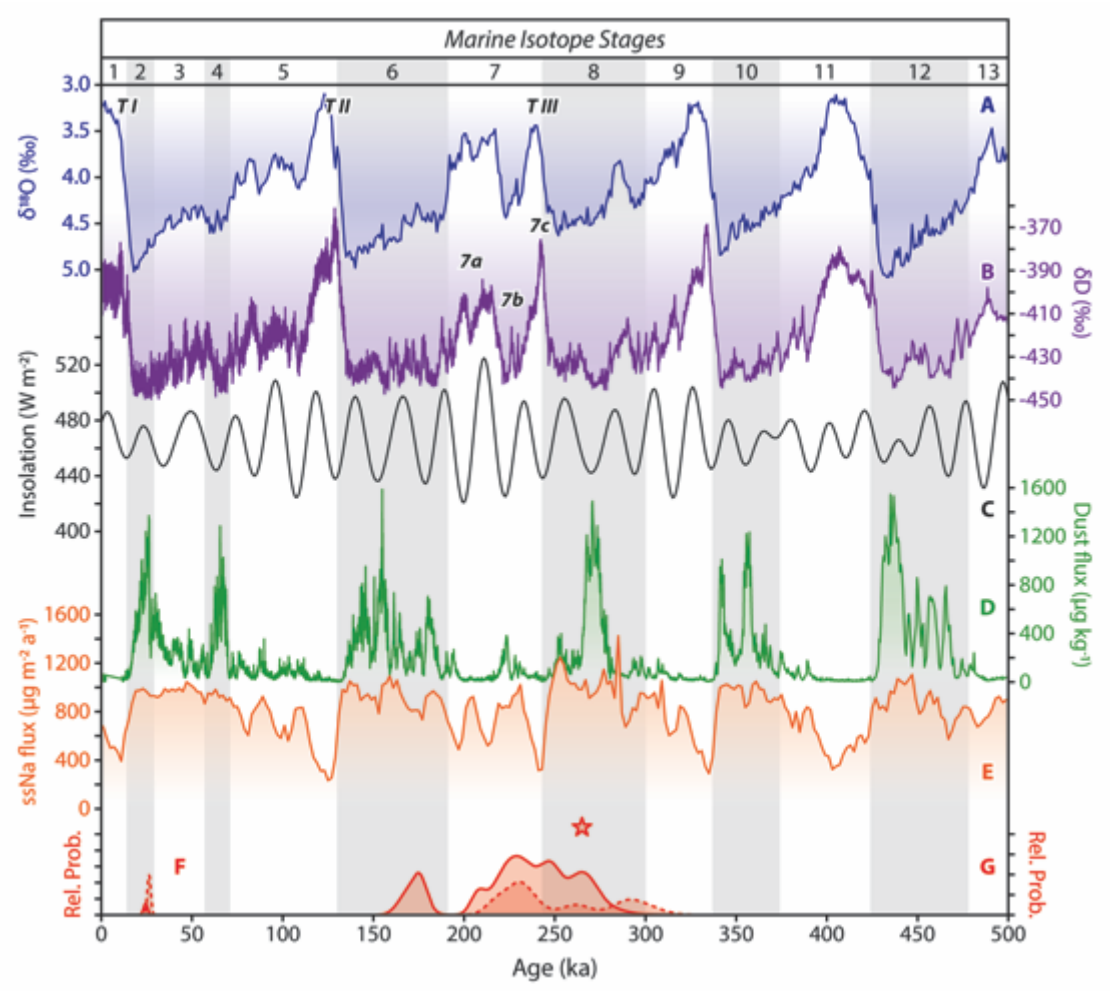

Figure 9. A comparison of the timing of outwash deposition in LBA and LP with a range of palaeoclimate proxies. (A) The LR04 benthic foraminiferal stack (Lisiecki and Raymo, 2005), which is essentially a proxy for northern hemisphere ice volume. (B) Deuterium record from the Antarctic EPICA Dome C ice core as a proxy for Southern Hemisphere temperature changes (Jouzel et al., 2007). (C) Summer (December) insolation intensity at 50˚S (Berger and Loutre, 1991). (D) Aeolian dust flux record from the EPICA Dome C ice core (Lambert et al., 2008). (E) Sea salt Na flux as a proxy for Antarctic sea ice variability (Wolff et al., 2006). (F and G) Our ^{10}Be data for outwash cobbles from LBA (solid lines) and LP (dashed lines) for the Fenix and Río Blanco limits (F) and Moreno and Hatcher limits (G), respectively (F and G plotted on separate relative probability scales). The star shows the timing of Moreno deposition at 260-270 ka. Also shown are the timings of glacial terminations (TI to TIII) and MIS 7a-c, mentioned in the text. The vertical bands correspond with marine isotope stages.

1093

References

.

Ackert, R.P., Mukhopadhyay, S., 2005. Constraining landform erosion and ages from surface exposure age distributions on old Patagonian moraines. Geochimica et Cosmochimica Acta 69, A162.

Ackert, R.P., Singer, B.S., Guillou, H., Kaplan, M.R., Kurz, M.D., 2003. Long-term cosmogenic He-3 production rates from Ar-40/Ar-39 and K-Ar dated Patagonian lava flows at 47 degrees S. Earth Planet. Sci. Lett. 210, 119-136.

Anderson, R.S., Duhnforth, M., Colgan, W., Anderson, L., 2012. Far-flung moraines: Exploring the feedback of glacial erosion on the evolution of glacier length. Geomorphology 179, 269-285.

Applegate, P.J., Urban, N.M., Keller, K., Lowell, T.V., Laabs, B.J.C., Kelly, M.A., Alley, R.B., 2012. Improved moraine age interpretations through explicit matching of geomorphic process models to cosmogenic nuclide measurements from single landforms. Quat. Res. 77, 293-304.

Bagnold, R.A., 1941. The Physics of Blown Sand and Desert Dunes. Chapman Hall, London.

Balco, G., 2011. Contributions and unrealized potential contributions of cosmogenic-nuclide exposure dating to glacier chronology, 1990-2010. Quat. Sci. Rev. 30, 3-27.

Balco, G., Stone, J.O., Lifton, N.A., Dunai, T.J., 2008. A complete and easily accessible means of calculating surface exposure ages or erosion rates from Be-10 and Al-26 measurements. Quaternary Geochronology 3, 174-195.

Basile, I., Grousset, F.E., Revel, M., Petit, J.R., Biscaye, P.E., Barkov, N.I., 1997. Patagonian origin of glacial dust deposited in East Antarctica (Vostok and Dome C) during glacial stages 2, 4 and 6. Earth Planet. Sci. Lett. 146, 573-589.

Berger, A., Loutre, M.F., 1991. INSOLATION VALUES FOR THE CLIMATE OF THE LAST 10000000 YEARS. Quat. Sci. Rev. 10, 297-317.

Bierman, P.R., Caffee, M.W., Davis, P.T., Marsella, K., Pavich, M., Colgan, P., Mickelson, D., Larsen, J., 2002. Rates and timing of earth surface processes from in situ-produced cosmogenic Be-10, Beryllium: Mineralogy, Petrology, And Geochemistry. Mineralogical Soc America, Washington, pp. 147-205.

Blunier, T., Brook, E.J., 2001. Timing of millennial-scale climate change in Antarctica and Greenland during the last glacial period. Science 291, 109-112.

Blunier, T., Schwander, J., Stauffer, B., Stocker, T., Dallenbach, A., Indermuhle, A., Tschumi, J., Chappellaz, J., Raynaud, D., Barnola, J.M., 1997. Timing of the Antarctic cold reversal and the atmospheric CO2 increase with respect to the Younger Dryas event. Geophysical Research Letters 24, 2683-2686.

Borchers, B., Marrero, S., Balco, G., Caffee, M., Goehring, B., Lifton, N., Nishiizumi, K., Phillips, F., Schaefer, J., Stone, J., 2016. Geological calibration of spallation production rates in the CRONUS-Earth project. Quaternary Geochronology 31, 188-198.

Caldenius, C.R.C., 1932. Las glaciaciones cuaternarias en la Patagonia y Tierra del Fuego : una investigación regional, estratigráfica y geocronológica : una comparación con la escala geocronológica sueca : with an English summary. [Stockholms högskola], Stockholm.

Carrasco, J.F., Casassa, G., Rivera, A., 2002. Meteorological and Climatological Aspects of the Southern Patagonia Icefield, in: Casassa, G., Sepúlveda, F.V., Sinclair, R.M. (Eds.), The Patagonian Icefields: A Unique Natural Laboratory for Environmental and Climate Change Studies. Springer US, Boston, MA, pp. 29-41.

1143 Chorley, R.J., Schumm, S.A., Sugden, D.E., 1984. Geomorphology, Methuen,
1144 London, New-York.
1145 Christl, M., Vockenhuber, C., Kubik, P.W., Wacker, L., Lachner, J., Alfimov, V.,
1146 Synal, H.A., 2013. The ETH Zurich AMS facilities: Performance parameters and
1147 reference materials. Nuclear Instruments and Methods in Physics Research Section B:
1148 Beam Interactions with Materials and Atoms 294, 29-38.
1149 Clapperton, C.M., 1993. Quaternary Geology and Geomorphology of South America.
1150 Elsevier Science Publishers B. V., Amsterdam.
1151 Coronato, A., Martinez, O., Rabassa, J., 2004. Glaciations in Argentine Patagonia,
1152 southern South America in: Ehlers, J., Gibbard, P.L. (Eds.), Quaternary Glaciations –
1153 Extent and Chronology, Part III. Elsevier, London, pp. 49-67.
1154 Darvill, C.M., Bentley, M.J., Stokes, C.R., 2015a. Geomorphology and weathering
1155 characteristics of erratic boulder trains on Tierra del Fuego, southernmost South
1156 America: Implications for dating of glacial deposits. Geomorphology 228, 382-397.
1157 Darvill, C.M., Bentley, M.J., Stokes, C.R., Hein, A.S., Rodes, A., 2015b. Extensive
1158 MIS 3 glaciation in southernmost Patagonia revealed by cosmogenic nuclide dating of
1159 outwash sediments. Earth Planet. Sci. Lett. 429, 157-169.
1160 Darvill, C.M., Bentley, M.J., Stokes, C.R., Shulmeister, J., 2016. The timing and
1161 cause of glacial advances in the southern mid-latitudes during the last glacial cycle
1162 based on a synthesis of exposure ages from Patagonia and New Zealand. Quat. Sci.
1163 Rev. 149, 200-214.
1164 Delmonte, B., Basile-Doelsch, I., Petit, J.R., Maggi, V., Revel-Rolland, M., Michard,
1165 A., Jagoutz, E., Grousset, F., 2004. Comparing the Epica and Vostok dust records
1166 during the last 220,000 years: stratigraphical correlation and provenance in glacial
1167 periods. Earth-Science Reviews 66, 63-87.
1168 Denton, G.H., Heusser, C.J., Lowell, T.V., Moreno, P.I., Andersen, B.G., Heusser,
1169 L.E., Schluchter, C., Marchant, D.R., 1999a. Interhemispheric linkage of paleoclimate
1170 during the last glaciation. Geogr. Ann. Ser. A-Phys. Geogr. 81A, 107-153.
1171 Denton, G.H., Hughes, T.J., 1983. Milankovitch Theory Of Ice Ages - Hypothesis Of
1172 Ice-Sheet Linkage Between Regional Insolation And Global Climate. Quat. Res. 20,
1173 125-144.
1174 Denton, G.H., Lowell, T.V., Heusser, C.J., Schluchter, C., Andersen, B.G., Heusser,
1175 L.E., Moreno, P.I., Marchant, D.R., 1999b. Geomorphology, stratigraphy, and
1176 radiocarbon chronology of Llanquihue drift in the area of the southern Lake District,
1177 Seno Reloncavi, and Isla Grande de Chiloe, Chile. Geogr. Ann. Ser. A-Phys. Geogr.
1178 81A, 167-229.
1179 Douglass, D.C., Bockheim, J.G., 2006. Soil-forming rates and processes on
1180 Quaternary moraines near Lago Buenos Aires, Argentina. Quat. Res. 65, 293-307.
1181 Douglass, D.C., Singer, B., Ackert, R.P., Stone, J., Kaplan, M.R., Caffee, M., 2007.
1182 Constraining boulder erosion rates and ages of mid-Pleistocene moraines, Lago
1183 Buenos Aires, Argentina. GSA Abstracts and Programs Northeastern Section - 42nd
1184 Annual Meeting.
1185 Douglass, D.C., Singer, B.S., Kaplan, M.R., Ackert, R.P., Mickelson, D.M., Caffee,
1186 M.W., 2005. Evidence of early Holocene glacial advances in southern South America
1187 from cosmogenic surface-exposure dating. Geology 33, 237-240.
1188 Douglass, D.C., Singer, B.S., Kaplan, M.R., Mickelson, D.M., Caffee, M.W., 2006.
1189 Cosmogenic nuclide surface exposure dating of boulders on last-glacial and late-
1190 glacial moraines, Lago Buenos Aires, Argentina: Interpretive strategies and
1191 paleoclimate implications. Quaternary Geochronology 1, 43-58.
1192 EPICA, 2004. Eight glacial cycles from an Antarctic ice core. Nature 429, 623-628.

1193 Garcia, J.L., Kaplan, M.R., Hall, B.L., Schaefer, J.M., Vega, R.M., Schwartz, R.,
1194 Finkel, R., 2012. Glacier expansion in southern Patagonia throughout the Antarctic
1195 cold reversal. Geology 40, 859-862.
1196 Garreaud, R., Lopez, P., Minvielle, M., Rojas, M., 2013. Large-Scale Control on the
1197 Patagonian Climate. Journal of Climate 26, 215-230.
1198 Glasser, N.F., Jansson, K.N., Harrison, S., Kleman, J., 2008. The glacial
1199 geomorphology and Pleistocene history of South America between 38 degrees S and
1200 56 degrees S. Quat. Sci. Rev. 27, 365-390.
1201 Hallet, B., Putkonen, J., 1994. Surface Dating Of Dynamic Landforms - Young
1202 Boulders On Aging Moraines. Science 265, 937-940.
1203 Hays, J.D., Imbrie, J., Shackleton, N.J., 1976. Variations In Earths Orbit - Pacemaker
1204 Of Ice Ages. Science 194, 1121-1132.
1205 Hein, A.S., Dunai, T.J., Hulton, N.R.J., Xu, S., 2011. Exposure dating outwash
1206 gravels to determine the age of the greatest Patagonian glaciations. Geology 39, 103-
1207 106.
1208 Hein, A.S., Hulton, N.R.J., Dunai, T.J., Kaplan, M.R., Sugden, D., Xu, S., 2010. The
1209 chronology of the Last Glacial Maximum and deglacial events in central Argentine
1210 Patagonia. Quat. Sci. Rev.
1211 Hein, A.S., Hulton, N.R.J., Dunai, T.J., Schnabel, C., Kaplan, M.R., Naylor, M., Xu,
1212 S., 2009. Middle Pleistocene glaciation in Patagonia dated by cosmogenic-nuclide
1213 measurements on outwash gravels. Earth Planet. Sci. Lett. 286, 184-197.
1214 Herman, F., Brandon, M., 2015. Mid-latitude glacial erosion hotspot related to
1215 equatorial shifts in southern Westerlies. Geology 43, 987-990.
1216 Heyman, J., Applegate, P.J., Blomdin, R., Gribenski, N., Harbor, J.M., Stroeven, A.P.,
1217 2016. Boulder height - exposure age relationships from a global glacial Be-10
1218 compilation. Quaternary Geochronology 34, 1-11.
1219 Heyman, J., Stroeven, A.P., Harbor, J.M., Caffee, M.W., 2011. Too young or too old:
1220 Evaluating cosmogenic exposure dating based on an analysis of compiled boulder
1221 exposure ages. Earth Planet. Sci. Lett. 302, 71-80.
1222 Hulton, N., Sugden, D., Payne, A., Clapperton, C., 1994. Glacier modeling and the
1223 climate of patagonia during the last glacial maximum. Quaternary Research (Orlando)
1224 42, 1-19.
1225 Hulton, N.R.J., Purves, R.S., McCulloch, R.D., Sugden, D.E., Bentley, M.J., 2002.
1226 The Last Glacial Maximum and deglaciation in southern South America. Quat. Sci.
1227 Rev. 21, 233-241.
1228 Imbrie, J., Berger, A., Boyle, E.A., Clemens, S.C., Duffy, A., Howard, W.R., Kukla,
1229 G., Kutzbach, J., Martinson, D.G., McIntyre, A., Mix, A.C., Molfino, B., Morley, J.J.,
1230 Peterson, L.C., Pisias, N.G., Prell, W.L., Raymo, M.E., Shackleton, N.J., Toggweiler,
1231 J.R., 1993. On The Structure And Origin Of Major Glaciation Cycles .2. The 100,000-
1232 Year Cycle. Paleoceanography 8, 699-735.
1233 Jouzel, J., Masson-Delmotte, V., Cattani, O., Dreyfus, G., Falourd, S., Hoffmann, G.,
1234 Minster, B., Nouet, J., Barnola, J.M., Chappellaz, J., Fischer, H., Gallet, J.C., Johnsen,
1235 S., Leuenberger, M., Loulergue, L., Luethi, D., Oerter, H., Parrenin, F., Raisbeck, G.,
1236 Raynaud, D., Schilt, A., Schwander, J., Selmo, E., Souchez, R., Spahni, R., Stauffer,
1237 B., Steffensen, J.P., Stenni, B., Stocker, T.F., Tison, J.L., Werner, M., Wolff, E.W.,
1238 2007. Orbital and millennial Antarctic climate variability over the past 800,000 years.
1239 Science 317, 793-796.
1240 Kaplan, M.R., Ackert, R.P., Singer, B.S., Douglass, D.C., Kurz, M.D., 2004.
1241 Cosmogenic nuclide chronology of millennial-scale glacial advances during O-isotope
1242 stage 2 in Patagonia. Geol. Soc. Am. Bull. 116, 308-321.

1243 Kaplan, M.R., Coronato, A., Hulton, N.R.J., Rabassa, J.O., Kubik, P.W., Freeman, S.,
1244 2007. Cosmogenic nuclide measurements in southernmost South America and
1245 implications for landscape change. Geomorphology 87, 284-301.
1246 Kaplan, M.R., Douglass, D.C., Singer, B.S., Caffee, M.W., 2005. Cosmogenic nuclide
1247 chronology of pre-last glacial maximum moraines at Lago Buenos Aires, 46 degrees
1248 S, Argentina. Quat. Res. 63, 301-315.
1249 Kaplan, M.R., Hein, A.S., Hubbard, A., Lax, S.M., 2009. Can glacial erosion limit the
1250 extent of glaciation? Geomorphology 103, 172-179.
1251 Kaplan, M.R., Strelin, J.A., Schaefer, J.M., Denton, G.H., Finkel, R.C., Schwartz, R.,
1252 Putnam, A.E., Vandergoes, M.J., Goehring, B.M., Travis, S.G., 2011. In-situ
1253 cosmogenic (10)Be production rate at Lago Argentino, Patagonia: Implications for
1254 late-glacial climate chronology. Earth Planet. Sci. Lett. 309, 21-32.
1255 Kohl, C.P., Nishiizumi, K., 1992. Chemical isolation of quartz for measurement of in
1256 situ-produced cosmogenic nuclides. Geochimica et Cosmochimica Acta 56, 3583-
1257 3587.
1258 Kubik, P.W., Christl, M., 2010. Be-10 and Al-26 measurements at the Zurich 6 MV
1259 Tandem AMS facility. Nuclear Instruments & Methods in Physics Research Section
1260 B-Beam Interactions with Materials and Atoms 268, 880-883.
1261 Lagabrielle, Y., Suarez, M., Malavieille, J., Morata, D., Espinoza, F., Maury, R.C.,
1262 Scalabrino, B., Barbero, L., de la Cruz, R., Rossello, E., Bellon, H., 2007. Pliocene
1263 extensional tectonics in the Eastern Central Patagonian Cordillera: geochronological
1264 constraints and new field evidence. Terra Nova 19, 413-424.
1265 Lagabrielle, Y., Suarez, M., Rossello, E.A., Herail, G., Martinod, J., Regnier, M., de
1266 la Cruz, R., 2004. Neogene to Quaternary tectonic evolution of the Patagonian Andes
1267 at the latitude of the Chile Triple Junction. Tectonophysics 385, 211-241.
1268 Lambert, F., Delmonte, B., Petit, J.R., Bigler, M., Kaufmann, P.R., Hutterli, M.A.,
1269 Stocker, T.F., Ruth, U., Steffensen, J.P., Maggi, V., 2008. Dust-climate couplings
1270 over the past 800,000 years from the EPICA Dome C ice core. Nature 452, 616-619.
1271 Lamy, F., Kaiser, J., Ninnemann, U., Hebbeln, D., Arz, H.W., Stoner, J., 2004.
1272 Antarctic timing of surface water changes off Chile and Patagonian ice sheet
1273 response. Science 304, 1959-1962.
1274 Lisiecki, L.E., Raymo, M.E., 2005. A Pliocene-Pleistocene stack of 57 globally
1275 distributed benthic delta O-18 records. Paleoceanography 20.
1276 McCulloch, R.D., Fogwill, C.J., Sugden, D.E., Bentley, M.J., Kubik, P.W., 2005.
1277 Chronology of the last glaciation in central Strait of Magellan and Bahia Inutil,
1278 southernmost South America. Geogr. Ann. Ser. A-Phys. Geogr. 87A, 289-312.
1279 Meglioli, A., 1992. Glacial geology and chronology of southernmost Patagonia and
1280 Tierra del Fuego, Argentina and Chile. Lehigh University, Bethlehem, p. 298.
1281 Mercer, J.H., 1976. Glacial History Of Southernmost South-America. Quat. Res. 6,
1282 125-166.
1283 Merchel, S., Arnold, M., Aumaître, G., Benedetti, L., Bourlès, D.L., Braucher, R.,
1284 Alfimov, V., Freeman, S.P.H.T., Steier, P., Wallner, A., 2008. Towards more precise
1285 10Be and 36Cl data from measurements at the 10−14 level: Influence of sample
1286 preparation. Nuclear Instruments and Methods in Physics Research Section B: Beam
1287 Interactions with Materials and Atoms 266, 4921-4926.
1288 Moreno, P.I., Kaplan, M.R., Francois, J.P., Villa-Martinez, R., Moy, C.M., Stern,
1289 C.R., Kubik, P.W., 2009. Renewed glacial activity during the Antarctic cold reversal
1290 and persistence of cold conditions until 11.5 ka in southwestern Patagonia. Geology
1291 37, 375-378.

Mörner, N.A., Sylwan, C., 1989. Magnetostratigraphy of the Patagonian moraine sequence at Lago Buenos Aires. J. South Am. Earth Sci. 2, 385-389.
Nishiizumi, K., 2004. Preparation of Al-26 AMS standards. Nuclear Instruments & Methods in Physics Research Section B 223-24, 388-392.
Nishiizumi, K., Imamura, M., Caffee, M.W., Southon, J.R., Finkel, R.C., McAninch, J., 2007. Absolute calibration of Be-10 AMS standards. Nuclear Instruments & Methods in Physics Research Section B 258, 403-413.
Pedro, J.B., Bostock, H.C., Bitz, C.M., He, F., Vandergoes, M.J., Steig, E.J., Chase, B.M., Krause, C.E., Rasmussen, S.O., Markle, B.R., Cortese, G., 2016. The spatial extent and dynamics of the Antarctic Cold Reversal. Nature Geoscience 9, 51-+.
Phillips, F.M., Zreda, M.G., Smith, S.S., Elmore, D., Kubik, P.W., Sharma, P., 1990. Cosmogenic Chlorine-36 Chronology for Glacial Deposits at Bloody Canyon, Eastern Sierra-Nevada. Science 248, 1529-1532.
Phillips, R.J., Sharp, W.D., Singer, B.S., Douglass, D.C., 2006. Utilising U-series disequilibria of calcic soils to constrain the surface age of Quaternary deposits: A comparison with 10Be, 26 Al age data from Patagonian glacial moraines. Geochimica et Cosmochimica Acta 70, A491.
Prohaska, F., 1976. The climate of Argentina, Paraguay and Uruguay, in: W, S. (Ed.), Climates of Central and South America. Elsevier, Amsterdam, pp. 13-112.
Putkonen, J., O'Neal, M., 2006. Degradation of unconsolidated Quaternary landforms in the western North America. Geomorphology 75, 408-419.
Putkonen, J., Swanson, T., 2003. Accuracy of cosmogenic ages for moraines. Quat. Res. 59, 255-261.
Putnam, A.E., Schaefer, J.M., Denton, G.H., Barrell, D.J.A., Birkel, S.D., Andersen, B.G., Kaplan, M.R., Finkel, R.C., Schwartz, R., Doughty, A.M., 2013. The Last Glacial Maximum at 44 degrees S documented by a Be-10 moraine chronology at Lake Ohau, Southern Alps of New Zealand. Quat. Sci. Rev. 62, 114-141.
Rabassa, J., Clapperton, C.M., 1990. Quaternary Glaciations Of The Southern Andes. Quat. Sci. Rev. 9, 153-174.
Rabassa, J., Coronato, A., Bujalesky, G., Salemme, M., Roig, C., Meglioli, A., Heusser, C., Gordillo, S., Roig, F., Borromei, A., Quattrocchio, M., 2000. Quaternary of Tierra del Fuego, Southernmost South America: an updated review. Quat. Int. 68, 217-240.
Rabassa, J., Coronato, A., Martinez, O., 2011. Late Cenozoic glaciations in Patagonia and Tierra del Fuego: an updated review. Biological Journal of the Linnean Society 103, 316-335.
Scalabrino, B., Lagabrielle, Y., Malavieille, J., Dominguez, S., Melnick, D., Espinoza, F., Suarez, M., Rossello, E., 2010. A morphotectonic analysis of central Patagonian Cordillera: Negative inversion of the Andean belt over a buried spreading center? Tectonics 29, 27.
Schaefer, J.M., Putnam, A.E., Denton, G.H., Kaplan, M.R., Birkel, S., Doughty, A.M., Kelley, S., Barrell, D.J.A., Finkel, R.C., Winckler, G., Anderson, R.F., Ninneman, U.S., Barker, S., Schwartz, R., Andersen, B.G., Schluechter, C., 2015. The Southern Glacial Maximum 65,000 years ago and its Unfinished Termination. Quat. Sci. Rev. 114, 52-60.
Singer, B.S., Ackert, R.P., Guillou, H., 2004. Ar-40/Ar-19 and K-Ar chronology of Pleistocene glaciations in Patagonia. Geol. Soc. Am. Bull. 116, 434-450.
Smedley, R.K., Glasser, N.F., Duller, G.A.T., 2016. Luminescence dating of glacial advances at Lago Buenos Aires (similar to 46 degrees S), Patagonia. Quat. Sci. Rev. 134, 59-73.

Staiger, J., Gosse, J., Toracinta, R., Oglesby, B., Fastook, J., Johnson, J.V., 2007. Atmospheric scaling of cosmogenic nuclide production: Climate effect. Journal of Geophysical Research-Solid Earth 112.

Suárez, M., De La Cruz, R., 2001. Jurassic to miocene K-Ar dates from eastern central Patagonian Cordillera plutons, Chile (45 degrees-48 degrees S). Geological Magazine 138, 53-66.

Sugden, D.E., McCulloch, R.D., Bory, A.J.M., Hein, A.S., 2009. Influence of Patagonian glaciers on Antarctic dust deposition during the last glacial period. Nature Geoscience 2, 281-285.

Ton-That, T., Singer, B., Mörner, N., Rabassa, J., 1999. Datación de lavas basalticas por 40Ar/39Ar geología glacial de la region del lago Buenos Aires, provincia de Santa Cruz, Argentina. Revisita de la Asociación Geológica Argentina 54, 333-352.

Wolff, E.W., Fischer, H., Fundel, F., Ruth, U., Twarloh, B., Littot, G.C., Mulvaney, R., Rothlisberger, R., de Angelis, M., Boutron, C.F., Hansson, M., Jonsell, U., Hutterli, M.A., Lambert, F., Kaufmann, P., Stauffer, B., Stocker, T.F., Steffensen, J.P., Bigler, M., Siggaard-Andersen, M.L., Udisti, R., Becagli, S., Castellano, E., Severi, M., Wagenbach, D., Barbante, C., Gabrielli, P., Gaspari, V., 2006. Southern Ocean sea-ice extent, productivity and iron flux over the past eight glacial cycles. Nature 440, 491-496.

Xu, S., Freeman, S.P.H.T., Rood, D.H., Shanks, R.P., 2014. Al-26 interferences in accelerator mass spectrometry measurements. Nuclear Instruments & Methods in Physics Research Section B-Beam Interactions with Materials and Atoms 333, 42-45.

Xu, S., Freeman, S.P.H.T., Sanderson, D., Shanks, R.P., Wilcken, K.M., 2013. Cl can interfere with Al3+ AMS but B need not matter to Be measurement. Nuclear Instruments & Methods in Physics Research Section B-Beam Interactions with Materials and Atoms 294, 403-405.

Zentmire, K.N., Gosse, J., Baker, C., McDonald, E., Wells, S., 1999. The problem of inheritance when dating alluvial fans and terraces with TCN: Insight from the Matanuska Glacier. GSA Abstracts and Programs 31.

Zreda, M.G., Phillips, F.M., 1995. Insights into alpine moraine development from cosmogenic Cl-36 buildup dating. Geomorphology 14, 149-156.